COMMISSION
SIXTEENTH REGULAR SESSION
Port Moresby, Papua New Guinea
5 – 11 December 2019

REPORT ON ANALYSES OF THE 2016/2019 PNA FAD TRACKING PROGRAMME

WCPFC16-2019-IP06[1]
24 July 2019

[1] This paper was posted to SC15 meeting as **SC15-2019-MI-WP12**

SCIENTIFIC COMMITTEE

FIFTEENTH REGULAR SESSION

Pohnpei, Federated States of Micronesia

12-20 August 2019

Report on analyses of the 2016/2019 PNA FAD tracking programme

WCPFC-SC15-2019/MI-WP-12

Lauriane Escalle[1], Berry Muller[2], Joe Scutt Phillips[1], Stephen Brouwer[1], Graham Pilling [1] and the PNA Office

[1]Oceanic Fisheries Programme, The Pacific Community (SPC)

[2] Oceanic Division, Marshall Islands Marine Resources Authority (MIMRA)

Executive Summary

This paper presents analyses of the PNA's fish aggregating device (FAD) tracking programme including: a description of the data processing required; a description of the spatio-temporal distribution of buoy deployments and number of FADs at sea; FAD densities including a correction procedure using ocean-current driven simulations; matching positions within FAD tracking and VMS data; and an analysis of the fate of FADs. As FADs drift in the ocean, the associated electronics can be replaced making it difficult to follow individual FADs, therefore for the purposes of this analysis we followed the satellite buoys, unless otherwise stated.

To better distinguish drifting buoys from those on board vessels, data were analysed using a Random Forest model to identify the drifting at-sea section of each buoy trajectory, and at the same time identify deployment positions. In addition, as for previous years, the data received by PNA are modified by fishing companies prior to submission, for example information outside PNA Exclusive Economic Zones (EEZs) may be removed (i.e., "geo-fenced"), which could introduce a bias to the analyses. After undertaking the correction procedure, the filtered dataset consisted of 21.9 million transmissions from 41,000 unique buoys and covered the period from 1st January 2016 to 30th May 2019.

The number of deployments varied over time, with a total of 62,544 deployments from 2016–2019 (from 227 vessels including 140 buoy owner vessels and an additional 87 vessels where the fishing company was known, but the buoy ownership was not). The spatial distribution of deployments was very similar between observer data and FAD tracking data; both showed the main deployments areas to be in Kiribati south of the Gilberts Islands and Kiribati east of the Phoenix Islands, Nauru, and to the east of Papua New Guinea (PNG).

The number of transmissions from buoys almost doubled in 2017 (8.7 million compared to 4.5 in 2016), likely reflecting an increase in data provision rather than an increase in FADs. Then the number of transmissions kept increasing in the first few months of 2018 (maximum of 25,000 transmissions per day in 2017 to 30,000 transmissions per day at the beginning of 2018). However, from April 2018, a large drop in the number of transmissions occurred for unknown reasons. Nevertheless, the number of individual FAD buoys active has continually increased since 2016, with 10,918 buoys in 2016; 18,357 in 2017; and 20,319 in 2018. A decrease in both the number of transmissions and the number of FADs transmitting was detected during the FAD closure each year, with an unusual day-to-day variability detected in 2018. In addition, each year the number of transmissions and FADs transmitting dropped in December.

The average drift time and straight-line drift distance per FAD are 3 months and 1,033 km, whereas the average active time (including on-board sections) is 6 months with an average distance between first and last position of 1,617 km.

The raw spatial distribution of buoy densities was investigated, with higher densities in Kiribati south of the Gilbert Islands and around the Phoenix Islands, Tuvalu, PNG, and the Solomon Islands. However, this distribution clearly highlights the lack of FAD tracking data in some high seas areas due to issues related to geo-fencing. A simulation method, based on ocean currents, was therefore implemented to fill in the gaps in trajectories with missing sections. Corrected FAD densities could then be compiled

and used to further study the influence of FAD densities on the occurrence of associated and free school sets, CPUE, and catch per set.

Generalised additive models (GAMs) were fitted to evaluate the influence of various factors, in particular FAD densities, soak time and FAD characteristics, on the occurrence of associated and free school sets, CPUE and catch per set. The latter were derived from aggregated and corrected logsheet data (1° grid cell and monthly resolution); or observer data (at the set level, with daily FAD densities), which allowed access to additional variables (FAD characteristics, FAD drifting duration, moon phase, type of buoy and origin of FAD). The number of associated sets increased with FAD density, while skipjack, bigeye, yellowfin, and total CPUE showed a slight decrease with increasing FAD density. The analysis suggests that skipjack CPUE decreases with FAD densities above 180 per 1° cell per month. Similarly, CPUE from all unassociated sets slightly decreased with increasing FAD densities. GAM models, at the set level, also showed the influence of FAD drifting duration and FAD depth on catch per species.

Vessel VMS positions from five randomly selected vessels, were matched with FAD tracking data in 2018, based on date (±1h) and position (27.8km apart), with an actual visit to a FAD identified by at least five matching positions between a FAD and a vessel. This allowed the identification of deployment and setting activities.

Buoy positions at the end of their trajectories were investigated to study the fate of FADs, using a refined approach that considered that a FAD was lost when drifting outside the fishing ground of the company owning it (where the majority of that company's vessels were fishing). On that basis, 51.8% of FADs were classified as lost, 10.1% were retrieved; 6.7% were beached; 15.4% were sunk, stolen or had a malfunctioning buoy; and 14.0% were deactivated by the fishing company and left drifting, unmonitored at sea. In addition, the distance between the last position of lost FADs and core fishing ground of the company owning the FAD was 1,000–2,700 km, with an average of 2,000 km. Lost FADs were also found at a distance of 500–900 km from port, with an average of 750 km.

We invite WCPFC-SC15 to:

- Note this analysis on the PNA FAD tracking data and the progress being made by PNA in FAD tracking for the purpose of improving FAD management in PNA waters.
- Note the simulation method implemented to fill in the gaps in FAD trajectories and to compile corrected FAD densities maps. Furthermore, given the influence of FAD densities on CPUE, also note the key role that FAD densities may play in CPUE standardisation, but also in tuna behaviour as suggested in WCPFC-SC15-EB-WP-08. Hence, further note the importance of accessing FAD densities at the finest resolution possible for scientific analyses to guide management.
- Note the importance of complete FAD tracking data to support scientific analyses and encourage their provision by fishing companies.
- Note that findings of this paper highlighted that more than 50% of the FADs are lost to the fishing company owning it and that at least an additional 7% end up beached.

1. Introduction

The use of drifting Fish Aggregating Devices (FADs) by tropical tuna purse seiners has increased globally in the last few decades, particularly with the arrival of new technological developments to track FAD locations such as satellite and echo-sounder buoys (Fonteneau et al., 2013; Lopez et al., 2014). In the Western and Central Pacific Ocean (WCPO), the number of sets on artificial FADs has increased almost continuously since the 1990s and is currently more prevalent than sets on natural logs (Figure 1). In 2013, the number of FADs deployed in the WCPO was estimated at more than 30,000 per year (Gershman et al., 2015) and considered likely to have increased every year since. This was confirmed last year in a study that estimated that 30,700–64,900 were deployed annually in the WCPO in 2016 and 2017 (Escalle et al., 2018a). To reduce the impact of FAD fishing on tuna stocks, specifically due to the high capture of juvenile bigeye tuna on FAD associated sets (Harley et al., 2015), the Parties to the Nauru Agreement (PNA) and the Western and Central Pacific Fisheries Commission (WCPFC; hereafter 'the Commission') implemented a three to four month FAD closure, during which all FAD-related activities (e.g. fishing, deployment, servicing) are prohibited (i.e. CMM-2016-01). In addition, in 2018, the Commission implemented a limit of 350 FADs with activated instrumented buoys (activation on-board only) per vessel, at any given time (CMM-2017-01). Finally, to limit the impact of FADs on the marine ecosystem, the Commission also adopted measures to use low-entanglement risk FADs and to promote the use of biodegradable material on FADs (CMM 2018-01).

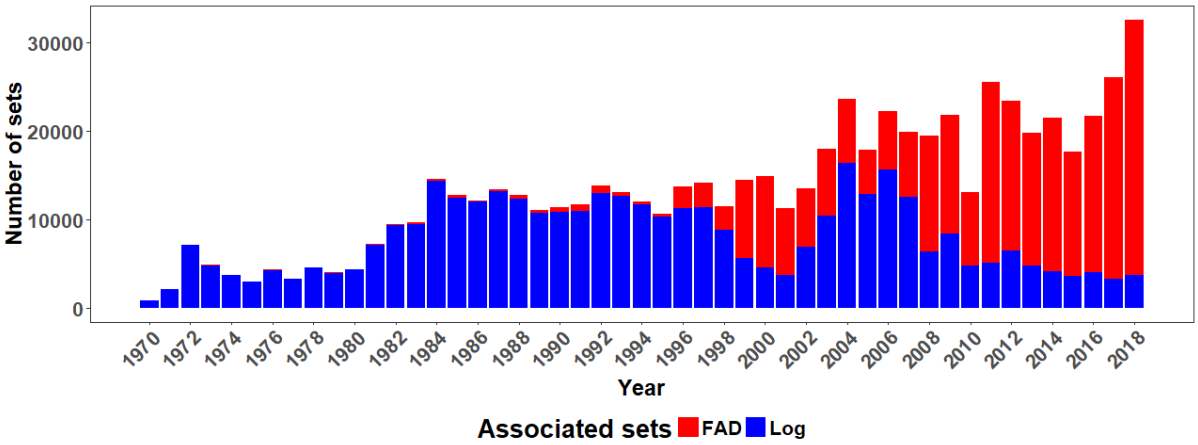

Figure 1. Number of associated sets performed specifically on deployed FADs and natural logs, as recorded in the aggregated logsheet data ("S-BEST" database: most complete dataset corrected for species composition, aggregated by 1° cell and month) in the Western and Central Pacific Ocean between 1979 and 2018. Similar trends were detected in the observer data but due to low coverage prior to 2010, these data are not shown.

This paper presents analyses of the PNA's FAD tracking programme, which tracked satellite buoys attached to drifting FADs used by purse seine vessels (Escalle et al., 2017b, 2018b). The aim was to improve the understanding of the use of FADs and their impacts. The scientific objectives of the programme are to:

a) improve our understanding of the use of FADs,
b) provide better scientific information on the impacts of FADs and fishing on them,
c) better understand the economics of FAD use, and
d) inform FAD management.

In this paper, we present the dataset and the processing method performed on the raw data. We also present results from analyses of i) spatio-temporal distributions of FAD buoy deployments; ii) the temporal distribution of drifting FADs in the WCPO; iii) FAD densities, including a simulation method to compile corrected FAD densities and then analyse their effect on catch per unit effort (CPUE); iv) matching positions within FAD tracking and vessel monitoring system (VMS) data; and v) the fate of FADs at their last buoy's transmission, including a focus on FAD beaching.

As FADs drift in the ocean, the associated electronics can be replaced making it difficult to follow individual FADs. Therefore, for the purposes of this analysis we followed FAD buoys with GPS satellite-positioning systems (referred hereafter as buoys), unless otherwise stated. Note that a buoy trajectory may not constitute a single FAD track, but rather can be a single buoy track that could have been moved between multiple FADs.

2. General description of the data

2.1 Data processing

The FAD tracking data comprise transmitted locations and time stamps from buoys attached to drifting FADs, between 1st January 2016 and 30th May 2019 (data uploaded on 1th of July 2019). The raw dataset included more than 22.9 million transmissions from 48,600 satellite buoys. Each transmission included location, time, the "fishing company" each FAD buoy belongs to (actual fishing company or directly a vessel name), water temperature, course direction, and drifting speed. However, the raw buoy tracking dataset received by the Parties to the Nauru Agreement Office (PNAO) contained duplications and errors, as well as transmissions from active buoys that were still on-board a vessel; therefore, the dataset needed to be filtered before any analysis could be undertaken (Escalle et al., 2017b, 2018b). The first filtering process was to remove buoys activated for short periods to verify functioning and avoid bias in the analyses due to very short overall active time. This included the removal of buoys with less than 10 transmissions, those active for less than seven days, and those with transmissions from only the same position (Table 1). In addition, double transmissions, consecutive transmissions corresponding to unrealistic speeds, as well as consecutive transmissions separated by more than three months at the end or beginning of a buoy track were removed. The filtered data set included 21,870,877 transmissions from 41,157 satellite buoys for analysis, corresponding to annual estimates of active buoys of 10,918 in 2016; 18,357 in 2017; 20,319 in 2018; and 9,980 in 2019 (Table 2).

Table 1. Summary information of the buoy tracking dataset showing the number (and %) of records removed during filtering processes.

	Number of transmissions	Number of buoys	% of transmissions	% of buoys
Raw dataset	**22,947,683**	**48,558**		
Buoy with ≤ 3 transmissions	100,784	2605	0.4	5.4
Double transmissions (same time and position)	865,356	0	3.8	0.0
Buoy with only one position	22,934	204	0.1	0.4
Buoy with only port position	2,880	18	0.0	0.0
Consecutive transmissions with high speed (>200 knots)	36,202	2	0.2	0.0
Buoy active ≤ 7 days or < 10 transmissions	33,852	4253	0.1	8.8
Buoy with total distance <10km	14,798	19	0.1	0.0
Total removed	1,076,806	7,101	4.7	14.6
Filter dataset	**21,870,877**	**41,457**		

Table 2. Statistics in the FAD tracking dataset per year.

Year	Number of transmissions	Number of FADs	Number of (re)deployments	% of echo-sounder buoys*
2016	4,466,778	10,918	14,922	76.5
2017	8,627,983	18,357	20,544	91.8
2018	6,846,253	20,319	20,613	97.1
2019	1,929,844	9,980	6,465	98.2

*For the buoys with known presence/absence of echo-sounder, i.e. 82.8% of the buoys in the dataset.

Secondly, additional processing of the data consisted of identifying at-sea and on-board positions of a buoy to avoid bias in analyses focusing on effective at-sea time of FADs (Escalle et al., 2017b; Maufroy et al., 2015). Transmissions start when a buoy is activated, which may be following deployment or a few hours to several days before deployment, and continued until deactivation (e.g. when a FAD is considered "lost" by the company, or is recovered). Each transmission was classified into an "at-sea" or "on-board" position following the method developed by Maufroy et al. (2015). First, a subset of the data was used to compile a learning dataset (1,060 buoys and 939,200 transmissions, i.e. 3.5% of the buoys when the method was first developed, i.e. Escalle et al., 2017b), for which at-sea and on-board positions were visually classified. This learning dataset was used to configure a Random Forest model and a cross validation procedure was implemented to check the performance of the model. The learning dataset was randomly split 100 times into a training dataset and a validation dataset, with 50% of the learning buoys in each dataset. Random Forest models were calibrated using the training datasets, then the class (at-sea or on-board) of positions in the validation datasets were predicted. Performance statistics (accuracy rate, Kappa statistic, specificity, sensitivity; see Maufroy et al. (2015) for details) were then generated. In addition, as Random Forest models consider each position independently, with no consideration of the prior or following positions, an additional correction procedure was needed to eliminate isolated or short at-sea or on-board sections surrounded by long on-board or at-sea positions. An additional statistic called segmentation rate was therefore added to account for this feature of the data. The correction procedure to reduce the segmentation rate consisted of i) changing to on-board positions, those sequences of one to three isolated at-sea positions; ii) changing to at-sea positions, those sequences of one to three isolated on-board positions with a speed <5 km/h; and iii) changing to on-board positions, those additional isolated sequences of at-sea positions lasting less than 24 hours. This additional correction procedure was selected as the preferred method after testing different correction procedures, and based on the statistics mentioned

above, combined with visual investigation of some buoys. Once the Random Forest model and the correction procedure were calibrated, it was then run over the entire filtered dataset. Each buoy track (i.e. trajectory) then consisted of one (69% of the FADs) or several drifting ("at-sea") segments (2–25 segments per FAD), separated by "on-board" positions. It was found that more than 50% (21,224) of the buoys had more than 50% of their transmissions at sea. Additionally, around 37% (15,357) of the buoys transmitted from sea 81–100% of the time. Generally, the transmission frequency was of once per hour or once per day per buoy (Figure 2).

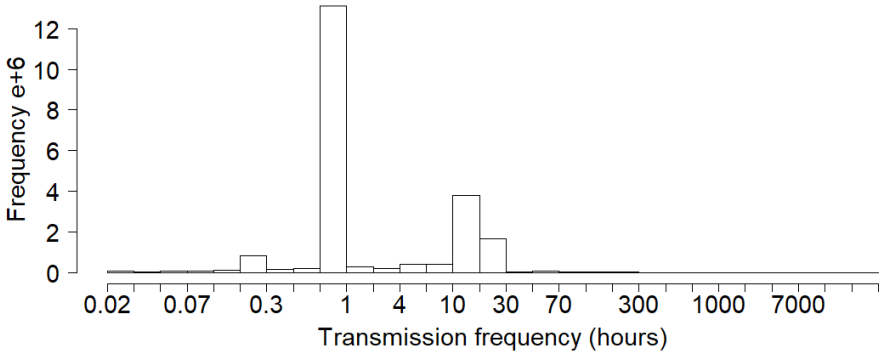

Figure 2. Frequency of transmission (in hours) for all buoys assessed from 2016– 2019.

Finally, the fishing company owner of each buoy with a vessel name recorded was added so that each buoy in the filtered dataset presented an actual fishing company and a vessel name when available (62% of the buoys with recorded vessel name, i.e. 140 vessels including 128 purse seiners and 12 support vessels). The type of buoy (e.g. echosounder or not) is not recorded, but from the format of the buoy manufacturer identification number (ID), it was deduced that at least 76.2% of the buoys are echo-sounder buoys (6.6% without and 17.2% unknown). Over the four years of the dataset, an increase in the use of satellite buoys with echo-sounder was detected, from 76.5% in 2016, 91.8% in 2017 and more than 97% in 2018 and 2019 (Table 2). Most of the buoys were manufactured by Satlink (63.0%) or Zunibal (19.8%).

2.2 Geo-fencing

The previously-identified systematic modification of buoy transmissions with information outside PNA EEZs being removed prior to data transmissions (i.e., "geo-fenced" FAD; see Figure 3 as an example) still occurred in 2018. Geo-fenced buoys were identified as having no transmitted positions outside PNA waters.

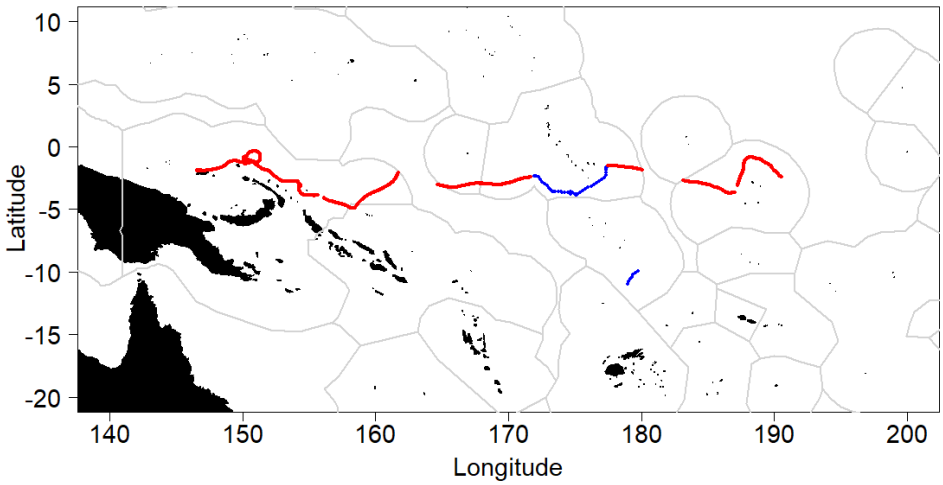

Figure 3. Example of a trajectory of a geo-fenced buoy, blue line represents on-board positions and red at-sea positions.

Patterns of buoys being geo-fenced by fishing companies prior to transmission to PNA appear variable between companies. Approximately 18% of the companies geo-fenced less than 25% of their FAD trajectories, while half were found to have geo-fenced their FAD data more than 75% percent of the time (Figure 4). Additionally, when FADs are geo-fenced it leads to gaps in the FAD trajectories of approximately a few days to one month (Escalle et al., 2018b), limiting the analyses performed on the data. Overall, a total of 27,961 FADs have been geo-fenced in 2016–2019.

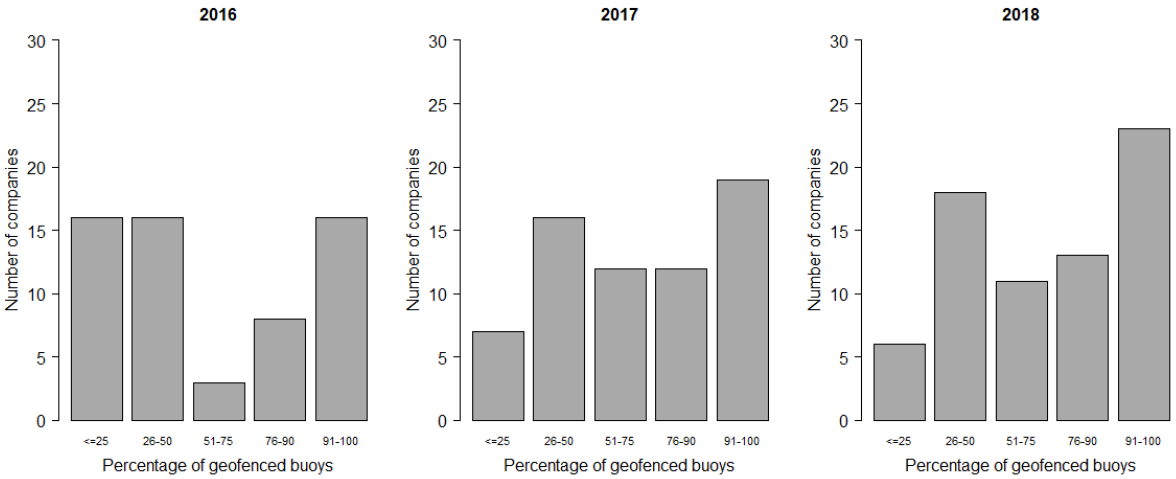

Figure 4. Percentage geo-fenced FAD buoys by company prior to transmission to PNA during 2016-2018. Given that the data for 2019 are incomplete, this year was not shown here.

Regarding temporal variability, besides the fact that few buoys were geo-fenced during the three first months of the programme, no temporal trends in the number of geo-fenced buoys by company could be determined (Figure 5). Since April 2016, between 63 and 93% of the FADs had been geo-fenced monthly (apart from December 2016 and 2017 when few FAD data were transmitted, and excluding the last three months with incomplete data).

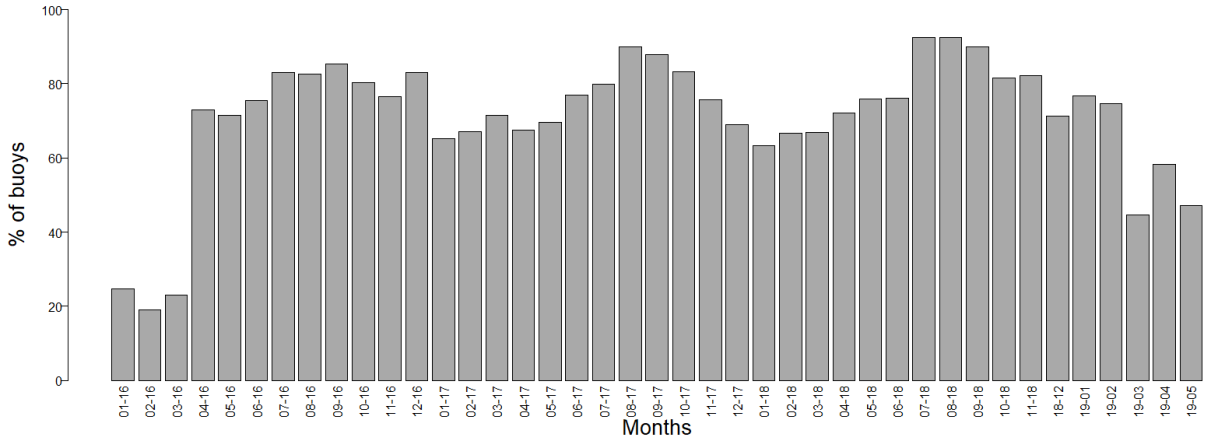

Figure 5. Percentage of geo-fenced buoys by month in 2016–2019.

We note that the geo-fencing of data supplied to the PNA affects many of the analyses described in this paper, including the identification of deployment events and locations (which may be outside PNA EEZs), estimation of FAD density (constrained to occur inside PNA EEZs only), soak time, the fate of FADs, etc., and hence also the scientific advice that can be provided to inform management options.

3. Deployments

The number of estimated buoy deployments varied over time (23 to 1,911 per week; Figure 6), with a total of 62,544 over the study period. This corresponds to 14,922; 20,544; 20,613 and 6,465 deployments in 2016, 2017, 2018 and 2019 respectively (Table 2; from 227 vessels linked to the FAD data; comprised of 140 identified FAD owner vessels and 87 additional vessels belonging to the identified fishing companies). Specifically, three peaks corresponding to the 1st week of January each year were identified, the first one corresponding to the beginning of the programme and the location of each buoy when the companies started transmitting data (i.e. not real deployments). The peaks in the beginning of 2017 and 2018 are plausible given the increase in buoy transmissions detected in Figure 9, but whether it corresponds to real deployments or to buoys already in the water that were activated/ reactivated at that time (only 24% of the buoys deployed the 1st week of 2017 were already active in 2016) or for which data only started to be transmitted to PNA, remains unclear. In addition to this bias in the deployments due to data beginning to be transmitted to PNA, another bias in the deployment positions arises from geo-fencing of the data, with 3.2% of the estimated deployments corresponding to the first position of a geo-fenced buoy appearing at the border of the PNA EEZs. Finally, the number of deployments decreased each year during the FAD closure, although a substantial number of deployments have still been identified during that period (Figure 6).

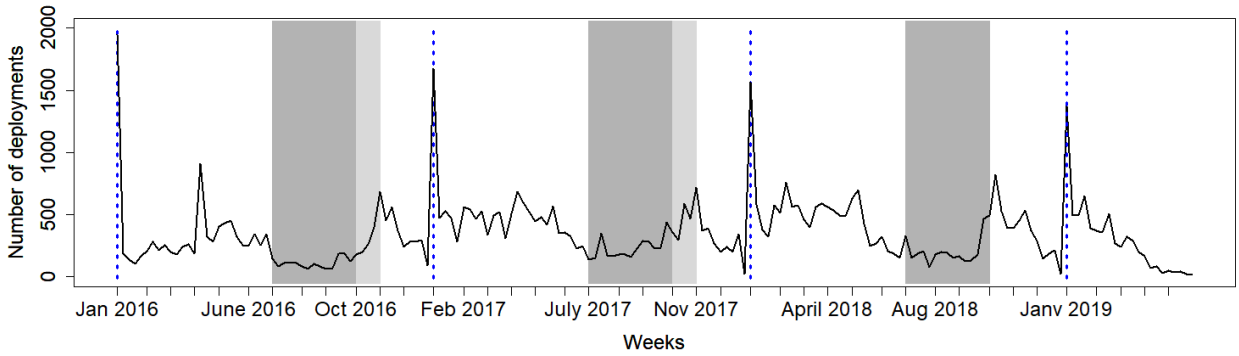

Figure 6. Estimated number of deployments by week. Grey areas correspond to the FAD-closure periods (1st of July through 30th of October or November).

Among the buoys with identified-owner vessels (227), the number of deployments per vessel was investigated (Figure 7). The total number of deployments by identifiable vessels in 2016–2018 (31,463 i.e. 56% of deployments) doubled from 5,528 in 2016 to 12,377 in 2017, and increased again in 2018 to 13,558, likely due to better data provision (Figure 7). Further, the number of deployments per vessel ranges from 0 to 286 in 2016 to 0 to 513 in 2017 and 0 to 414 in 2018.

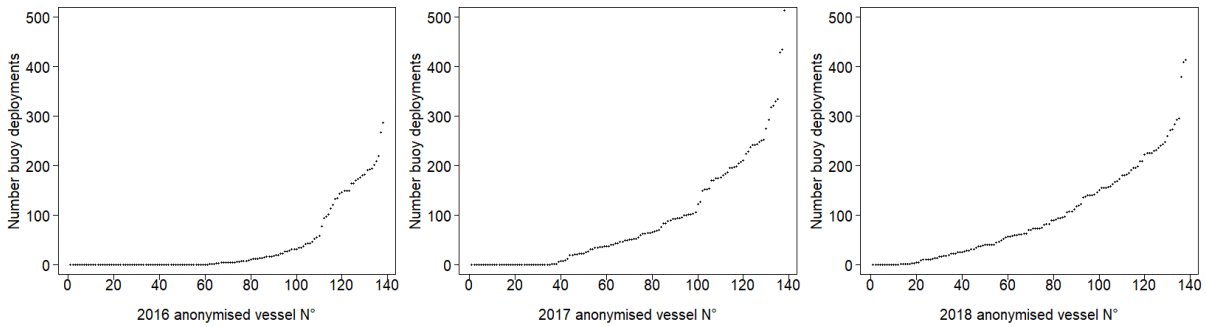

Figure 7. Estimated number of FAD buoy deployments for known vessels in the tracking data per year, 2016 (left), 2017(middle) and 2018 (right). Given that the data for 2019 are incomplete, this year was not shown here.

Over the three years of data (2016–2018), a large proportion of the deployments occurred in Kiribati south of the Gilbert Islands, north of Tuvalu and Nauru EEZs (Figure 8). In addition, for 2017 and 2018 a second hotspot of deployment was detected in Kiribati east of the Phoenix Islands EEZ (note that very few deployment were found within the Phoenix Islands Protected Area (PIPA), however the kriging method used tends to extend the hotspots artificially, linking them with other areas of high deployment). For example, deployments in the eastern high seas are in part an artefact of this, given the majority of data are geo-fenced. In the current dataset, deployments in the eastern high seas or FADs drifting from the Eastern Pacific Ocean (EPO) would appear as a deployment at the border of the Line Islands or at eastern boundary of the Marshall Islands and Gilbert Islands.

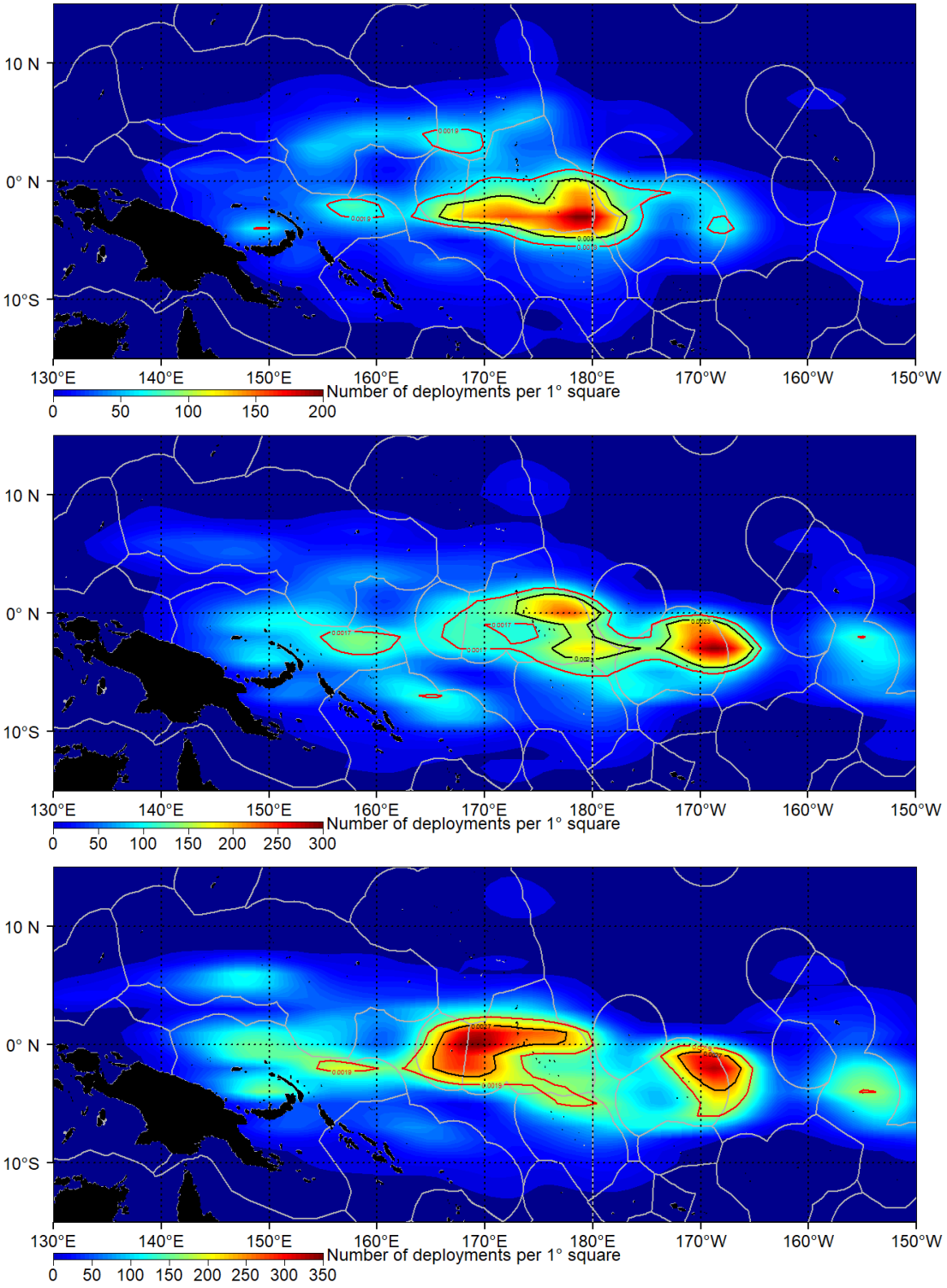

Figure 8. Smoothed kernel density of buoy deployments per 1° grid cell during 2016 (top), 2017 (middle) and 2018 (bottom). Red and black lines correspond to the 95th and 98th quantiles. Colour scale corresponds to the proportion of buoy deployment per 1° cell.

4. Temporal distribution of drifting FADs

4.1 Temporal variability in transmissions

The filtered dataset of 21,870,877 transmissions was comprised of 20% on-board positions and 80% at-sea positions. An increase in the number of transmissions and number of buoys transmitting within the data set was detected over time, linked to better data provision as mentioned previously (Figure 9). In particular, the number of transmissions from drifting buoys (at-sea) doubled in 2017 (8.7 million compared to 4.5 in 2016), and kept increasing in the first few months of 2018 (maximum of 25,000 transmissions per day in 2017 to 30,000 transmissions per day at the beginning of 2018). However, from April 2018, a large drop in the number of transmissions occurred for unknown reasons (15,000–20,000 transmissions per day before the closure, 0–20,000 during the FAD closure). Nevertheless, the number of individual FAD buoys active increased constantly since 2016, with 10,918 buoys in 2016, 18,357 in 2017, and 20,319 in 2018. Patterns of transmission changed during the period studied reflecting changes in reporting rates. For instance, a general increase in number of transmissions and number of buoys transmitting occurred in 2016; then both were relatively stable in 2018 compared to 2017 (except a decrease during the closure and at the end of the year). In 2018, unusual patterns were detected, the number of transmissions per day decreased after April 2018, while the number of buoys transmitting increased. In addition, during the closure, large day-to-day variability was detected. Additional years of data will be necessary to identify general patterns; however, a decrease in transmissions during the closure and at the end of the year was observed in all years.

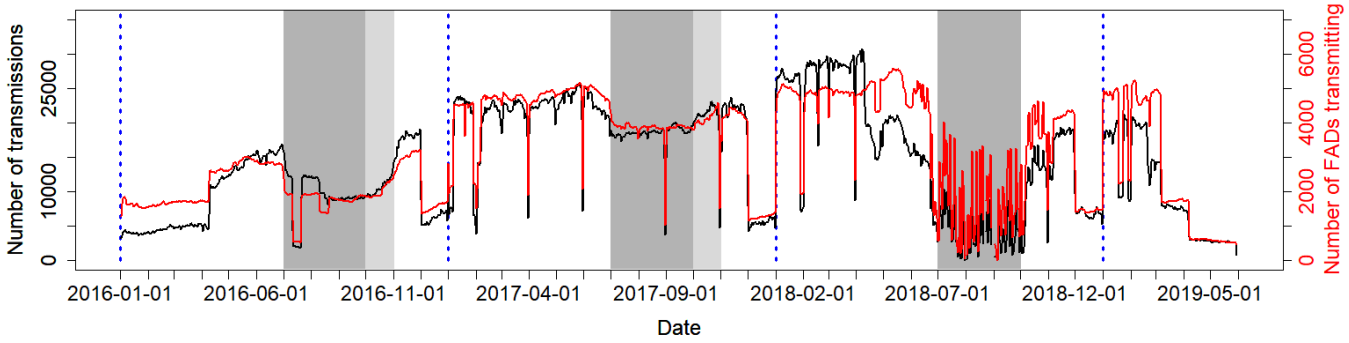

Figure 9. Number of transmissions (black line) and unique buoys transmitting (red line) daily from at-sea buoy positions only. Grey areas correspond to the FAD-closure periods (1st of July through 30th of September or October), and the blue lines denote January 1st.

Further investigation was undertaken to assess the change in transmission frequency in 2018 (Figure 10). As mentioned previously, the number of buoys transmitting remained similar to 2017, but a sharp decrease in the number of transmissions was detected from April 2018. This is due to the fact that most buoys transmitted only once per day, with a few buoys transmitting every hour (Figure 10). In 2017, most buoys were transmitting daily, while in 2018, many buoys had some days with no transmissions, particularly during the closure, when most buoys transmitted every two days or even less often (Figure 10).

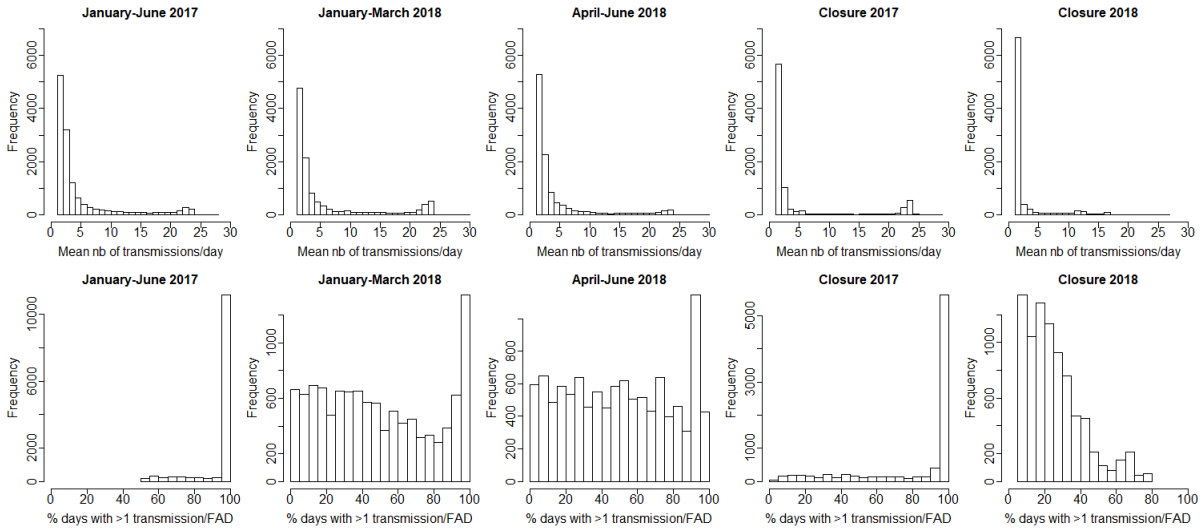

Figure 10. Distribution of the mean number (nb) of transmissions per FAD and per day (top) and percentage of days with more than one transmission per day per FAD (bottom).

4.2 Time and distance at sea

The longevity of FAD drifting and the linear distance drifted over that time were examined. Drifting at-sea times per FAD varied from less than 10 days to two years, with shorter times for buoys redeployed several times (Figure 11). The average drift time is around three months (95 days) with an average drift distance of 1,033 km, whereas the average active time (including on-board sections) was six months (180 days) with an average straight-line distance between first and last position of 1,617 km (Figure 12).

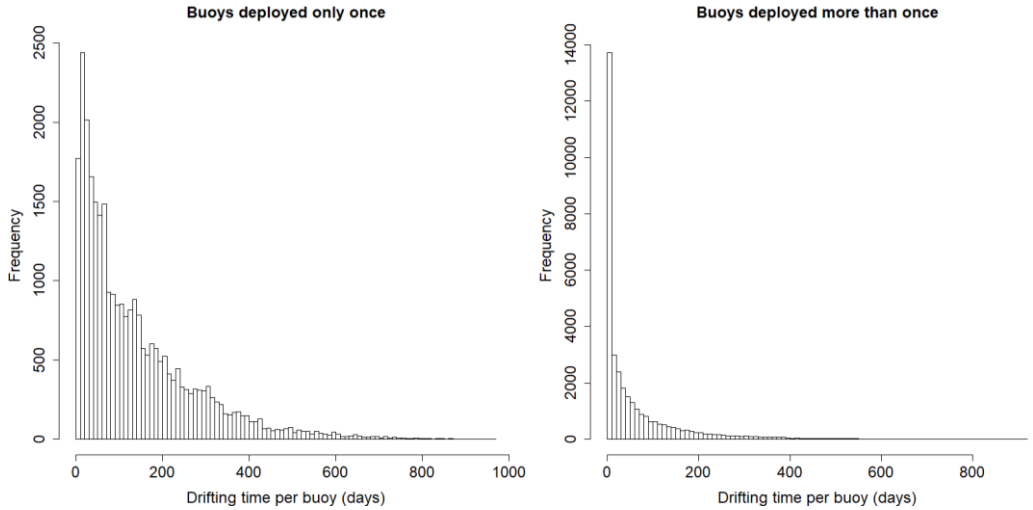

Figure 11. Drifting duration of FAD buoy tracks, for buoy deployed only once and buoys deployed at least one time (2016–2018).

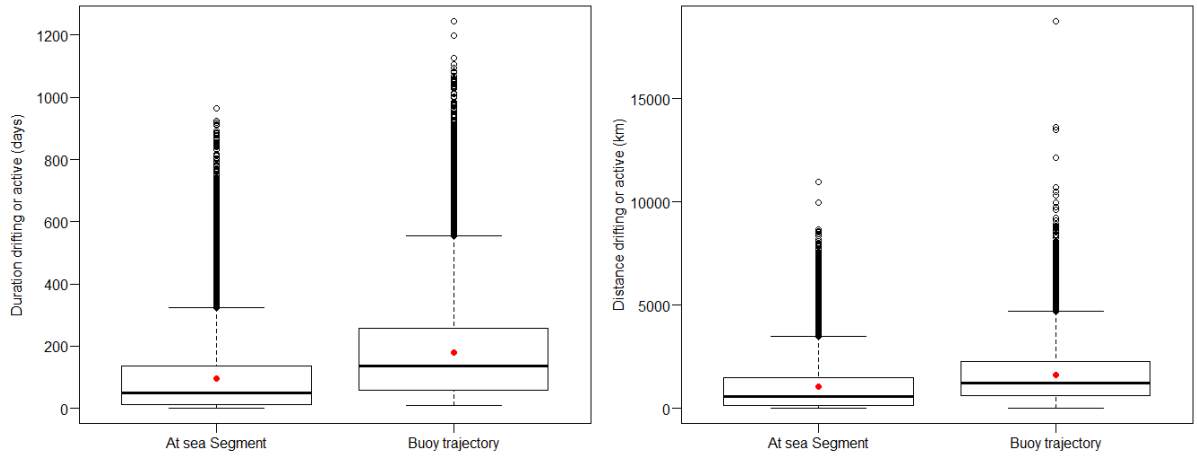

Figure 12. Duration (left) and distance (right) drifting per FAD buoy trajectory (whole buoy trajectory, including on-board segments) or at-sea segments (on-board segments removed).

Regarding the number of buoys per vessel, for buoys with identified owners (62%), vessels monitored one to 350 active buoys per day or per month (Figure 13). However, the majority of vessels had less than 150 active buoys per month and less than 100 per day. It should be noted that these statistics correspond to the data submitted by fishing companies to PNA, so they are likely underestimates of the true number of active buoys. In addition, these patterns represent the activity of only 128 purse seine vessels (out of 254 purse seiners in the logsheet data for 2016–2018).

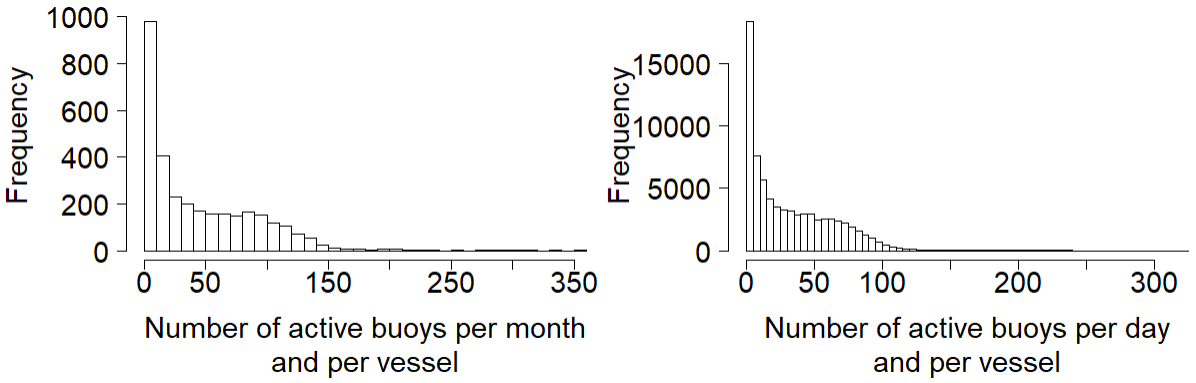

Figure 13. Histograms of the number of active buoys per month (left) or per day (right), per vessel (when vessel name was available) from 2016–2018, as recorded in the PNA FAD tracking data (see section 3.2. for estimated data submission rates).

5. FAD densities

5.1 Distribution of FAD densities

The distribution of drifting buoy density indicated areas with highest FAD density in Kiribati south of the Gilbert Islands and around the Phoenix Islands; Tuvalu (particularly in 2017 and 2018); Papua New Guinea; and the Solomon Islands (Figure 14).

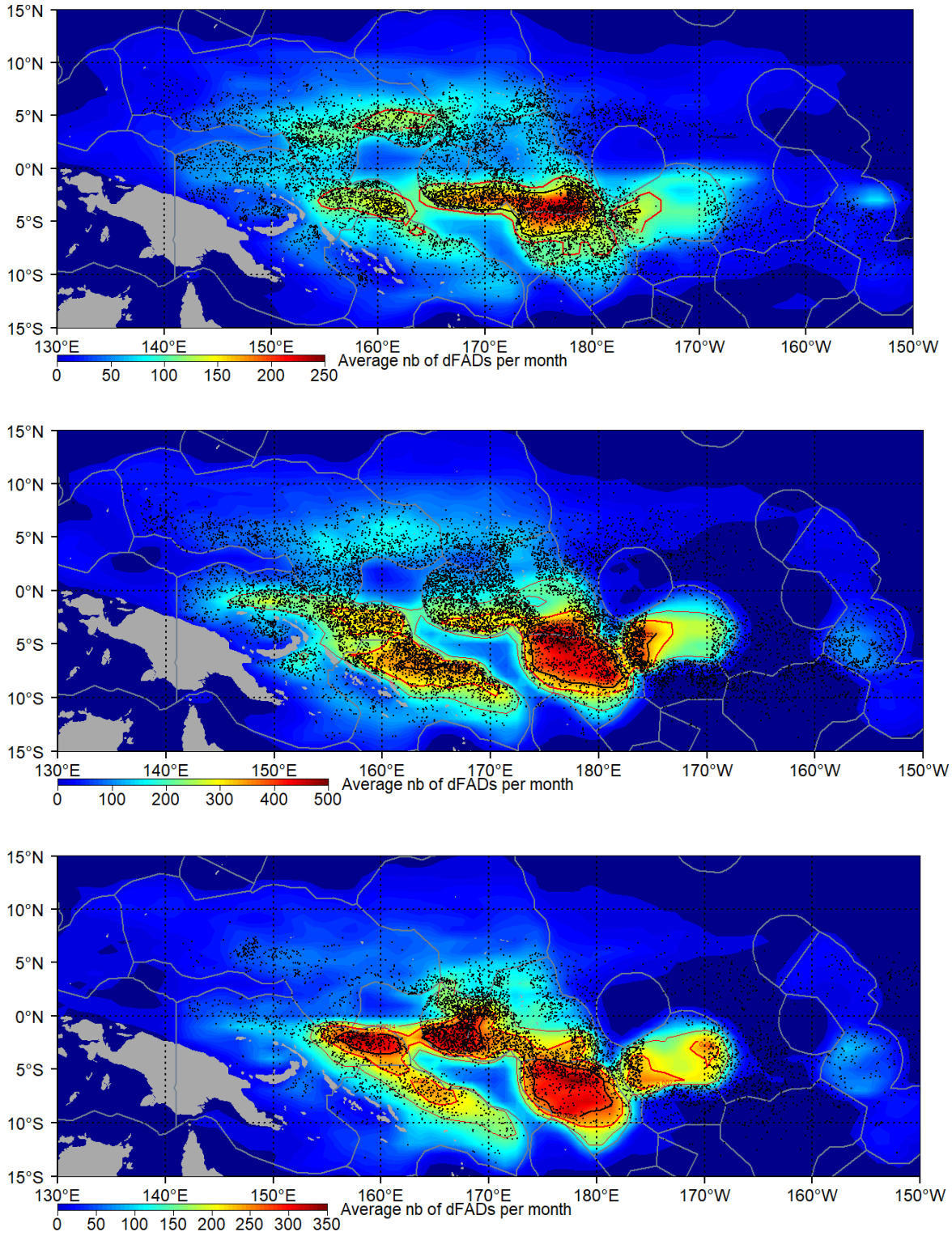

Figure 14. Smoothed kernel density of the average number (nb) of FAD satellite buoys transmitting at least once per month and per 1° grid cell during 2016 (top), 2017 (middle) and 2018 (bottom) with position of associated sets recorded in logsheet data shown as black dots. Red lines correspond to the 95th quantile. Colour scale corresponds to the average number of buoys transmitting per 1° cell per month.

Note that a temporal variability in FAD density distribution was detected through the course of the year, which may also be linked to the influence of the ENSO (El Niño–Southern Oscillation) cycle, as

these patterns were different between years. Lower transmission rates in 2016 may also have biased the observed FAD density.

Similar to the deployment maps, it is clear that we are missing some information due to geo-fencing and periods of non-transmission, with very low FAD densities in some areas outside PNA waters where some FAD sets are made. For instance, the southeast or northeast areas of the WCPO or the high seas between Tuvalu and Phoenix Islands EEZs. FAD density maps will be possible for a broader and more comprehensive spatial extent, likely suggesting higher FAD densities, once complete and unmodified FAD tracking data are obtained. Finally, we can clearly see the border of the PIPA, with no fishing sets within the reserve but a high density of FADs drifting through.

5.2. Corrected FAD densities based on oceanic currents

5.2.1 Simulation method

Lacking complete and unmodified FAD tracking data, we used a simulation method based on oceanic currents to interpolate FAD trajectories with missing sections (see Figure 3 as an example of a FAD presenting gaps in the trajectory). Missing sections may include positions outside PNA waters (i.e. geo-fenced FAD), but also additional missing information for unknown reasons. For instance, many FADs did not appear to transmit in December or at the end of certain months (Figure 9). Similarly, during the 2018 FAD closure, very high day-to-day variability was detected, with many FADs displaying gaps of several days in their trajectories (Figure 15). Gaps in trajectories vary from one day to more than six months (longer gaps were removed, as the likelihood that buoys would have been recovered and redeployed during that timeline is high). Besides the very short gaps (< 2 days), most missing sections were of less than 10 days (87,878 missing sections of 3–10 days in 20,150 buoys). In addition, FADs presenting their first position (1722 buoys) or their last position at a PNA border (2330) were also considered for the simulation approach, as the trajectory prior to or post PNA border is likely missing.

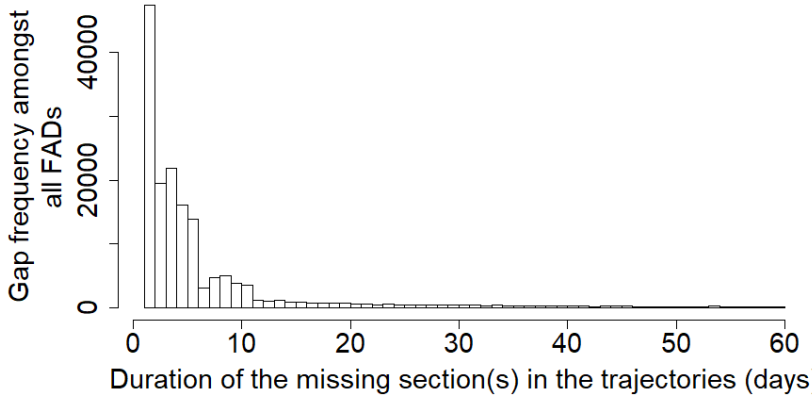

Figure 15. Histogram of the duration of the missing sections in FAD trajectories that were interpolated using the oceanic currents model. Missing sections of more than 60 days (N=4752) were removed from the histogram to increase interpretability.

To interpolate FAD trajectories during these missing sections, simulations were run using the *Parcels* Lagrangian simulation modelling framework (Lange and van Sebille, 2017), using a similar approach to that that has been used for simulated FADs previously (J Scutt Phillips et al., 2019). Particles (representing virtual FADs) were released at the last/first known position in the observed FAD

trajectory and then advected forward or backwards in time using flow fields based on an ocean circulation dataset. Ocean current data from the 1/12° HYCOM+NCODA Global Analysis (from the US Global Ocean Data Assimilation Experiment) were used, averaging current velocities over the top 50m of the ocean to reflect the median depth of FAD appendages in the WCPO (as recorded by observers; Escalle et al., 2017a). Ten particles were released for each simulation experiment (see below) and their positions were recorded every day over the simulated period (varying depending on the duration of the missing part of each FAD). To account for small scale variability not captured in the current forcing, small random displacements were added at each time step using a Brownian Motion model with a diffusivity constant of 10 m^2/s (Okubo, 1971; van Sebille et al., 2018).

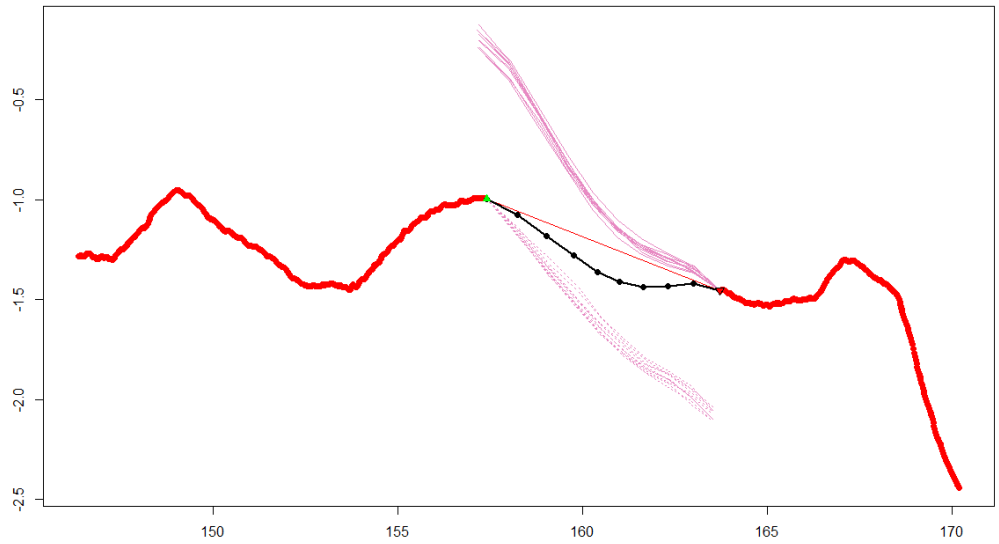

Figure 16. Example of a FAD trajectory with a missing section, shown as an orange straight line. The red dots indicate the observed at-sea trajectory of the FAD; pink lines the 10 forward and the 10 backward simulations; and the black dots and line the linear weighted daily position based on both forward and backward simulations.

In order to fill in the missing parts of trajectories described above, four types of simulations were performed. The two first simulations being use to deal with gaps in the dataset (specifically between PNA EEZs or not), while the second and third simulations are run independently to i) expand a trajectory backward in time that started, in the PNA dataset, at a PNA EEZ (third simulation); or ii) expand a trajectory forward in time that ended, in the PNA dataset, at a PNA EEZ (fourth simulation).

First, a simulation forcing particles forward in time was used to estimate the likely trajectory of the FAD from the last position recorded before a gap, lasting the duration of that missing section. Similarly, the second simulation, forcing particles backwards in time, estimated the likely trajectory before the first position at which the FAD reappears in the dataset after the missing section. The results from both of these simulations were used to estimate the likely position of the FAD every day during the missing section, using a linear weighted mean of the estimated positions of all particles in both simulations (Figure 16). Initial simulation experiments revealed that some slight altering of ocean flow fields is required to ensure no artificial beaching of simulated FADs that are known to have remained drifting, particularly during long periods of missing data. At present, a linear interpolation between the position after and before the gap, was performed for those simulations that resulted in spurious land interaction results. Similarly, a linear interpolation was also used for the short but more

numerous gaps of one and two days, due to limitations in computing power. As FADs are estimated to drift an average of 1/3 of degree per day, the linear interpolation for those short durations are sufficient to estimate FAD densities at a 1° grid cell resolution.

The third simulation consisted of simulating the backward drift trajectories of particles prior to their first recorded position at a PNA EEZ border. Finally, the fourth simulation forced particles forward in time following their last recorded position at a PNA EEZ border. It was decided to limit these two last simulations at 90 days, as we considered that longer simulations will unlikely reflect actual drift of the FADs, given the uncertainty in using ocean flow fields for Lagrangian simulation at these time-scales, and our uncertainty in the drift-time of the FAD. Finally, for each FAD with missing sections, the estimated daily position during each of the missing parts was compiled (Figure 17).

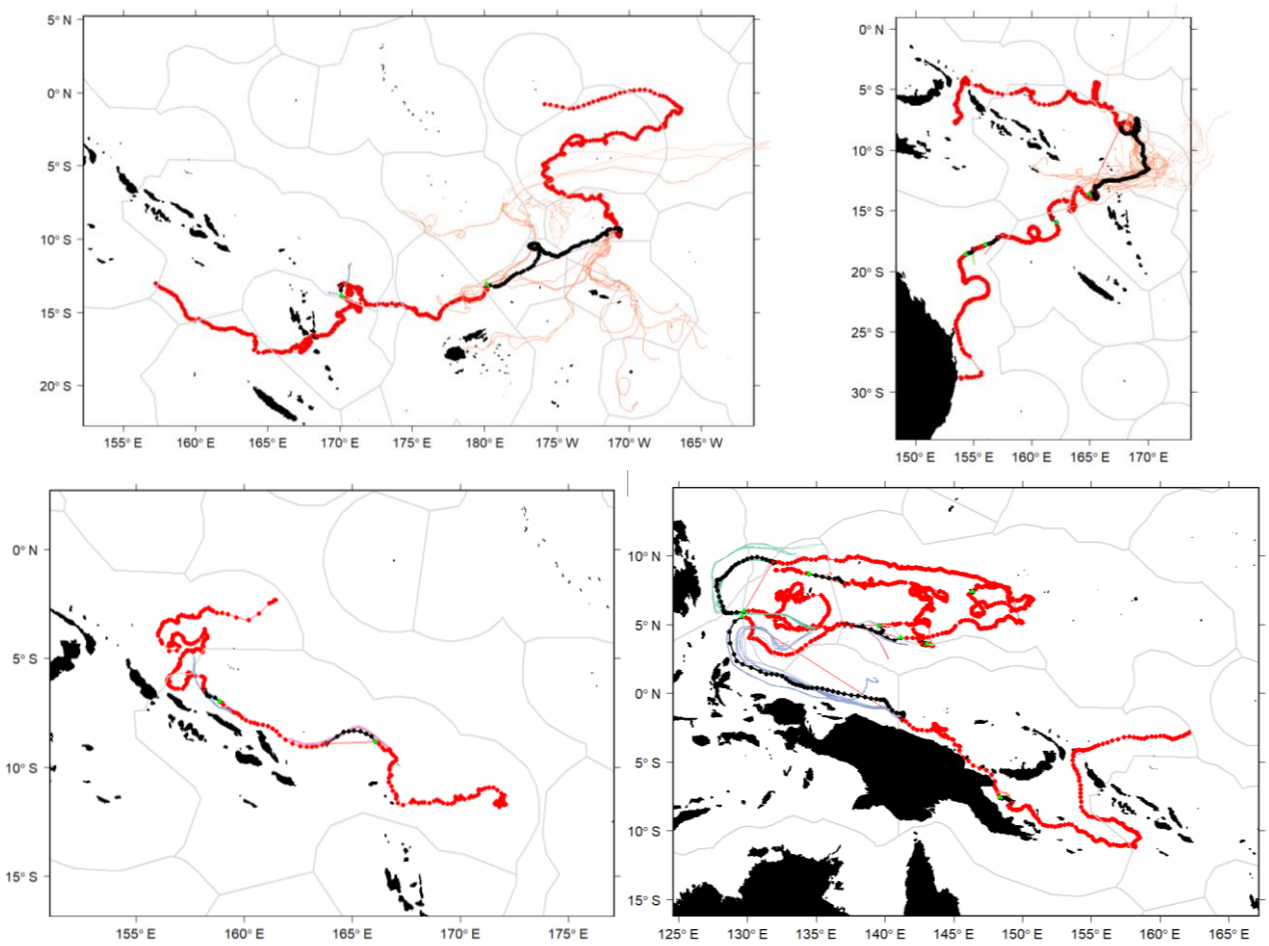

Figure 17. Examples of FAD tracks with gaps. Red dots indicate positions from the observed PNA FAD tracking data, while the black dots illustrate the estimated daily position during the missing sections using a Lagrangian simulation.

5.2.2 Results and corrected FAD densities

To investigate the temporal variability in the number of FADs in the WCPO, taking into account results from the simulations, we added the number of FADs per day from the simulations to the number of unique FADs transmitting per day (Figure 18). The corrected number of FADs per day shows a more stable pattern than before the correction using the simulations. For instance, the large dips in the time series that were observed at the end of some months, in December each year, or during the 2018 FAD

closure, are no longer occurring (except for December, but to a lesser extent; see Figure 18). Generally, an increase in the number of FADs represented in the dataset, each day, was detected from 2016 to 2017. However, this could again be simply due to higher transmission rates from fishing companies in the second year of the FAD tracking program (the simulation did not add FADs, but simply filled in the gaps in existing trajectories). Another increase was detected from 2017 to 2018, with a maximum daily number of FADs estimated at 7,000 in April 2018. Note however, that this would likely be underestimated, as it will be influence by the coverage rate of the data send by fishing companies. In particular, it has been estimated in previous reports that the amount of data transmitted to the PNA is of 30–40% (including missing sections from FADs in the dataset, but also FADs not present in the PNA FAD tracking dataset; Escalle et al., 2017b, 2018b). Hence, the number of FADs transmitting daily could be up to 2.5–3 times higher than the number estimated here. In addition, this would not account for FADs that have been deactivated, and do not transmit any satellite data. Finally, a small decrease in the number of FAD at sea is still detected during the closure each year (Figure 18).

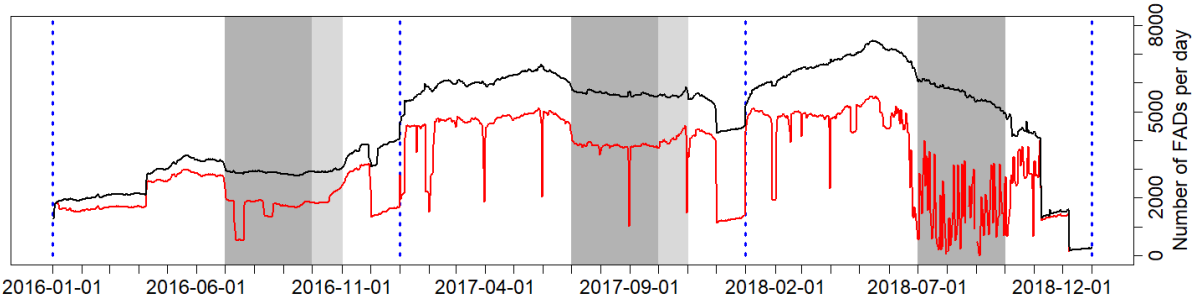

Figure 18. Total number of FAD buoys recorded per day in both the observed FAD tracking data (at-sea) and simulated data (black line) and number of FAD buoys transmitting per day in the FAD tracking data only (red line, as shown in Figure 9). Grey areas correspond to the FAD-closure periods (1st of July through 30th of September or October) and blue line January 1st.

The corrected trajectories of FADs were also used to compile corrected FAD densities (Figure 19). The correction procedure did not change the general distribution pattern of areas with higher FAD densities (e.g. Kiribati Gilbert Island, Kiribati Phoenix Island, Solomon Island and Tuvalu EEZ) but it increased the number of FADs detected in the high seas. This increase in FAD density in high seas areas is particularly noticeable in the high seas pocket between PNG, the Solomon Islands, Nauru, Kiribati Gilbert Islands and Tuvalu EEZ; as well as between Tuvalu and Kiribati Phoenix Islands. However, the level of FAD densities remain lower than in nearby areas (e.g. the border of Tuvalu and Solomon Islands EEZ). This would therefore indicate that additional correction or classification of missing trajectory sections may be needed to effectively estimate the FAD densities in these areas. We can also note that the general distribution of FAD densities is much larger in the corrected maps, with at least one FAD detected in almost every cell within the WCPO. This expanded FAD distribution would mainly be caused by the simulation of backward and forward drift of FADs that had their first or last position at the border of a PNA EEZ. Finally, we can also notice the connectivity between the Kiribati Line Island EEZ and the Phoenix Islands EEZ.

Some hypotheses may be formulated to explain the low densities in some high sea areas (e.g. high seas pockets) that still occur in the corrected FAD densities. The identification of geo-fenced trajectories is performed by checking if a buoy transmitted either first or last at a PNA border (simulations 3 and 4), and uses a buffer of 10km around the PNA EEZ border (5km in and out of the border). Subsequently, if these first or last positions were within a PNA EEZ, but outside this buffer,

the trajectories would not be identified as having been geo-fenced, and consequently simulated in our correction approach. For instance, this would include FADs deactivated or appearing within a PNA EEZ but at more than 5km from the border. This buffer around the PNA EEZ border is needed to identify geo-fencing, and should not be too wide and thus avoid simulating the trajectories of FADs effectively deployed or deactivated relatively close to the border. However, it would be relevant to vary the size of this buffer to examine the sensitivity to results. Finally, missing FADs in the corrected dataset could also be due to initially geo-fenced FADs, that have then been deactivated before ever reappearing in a PNA EEZ.

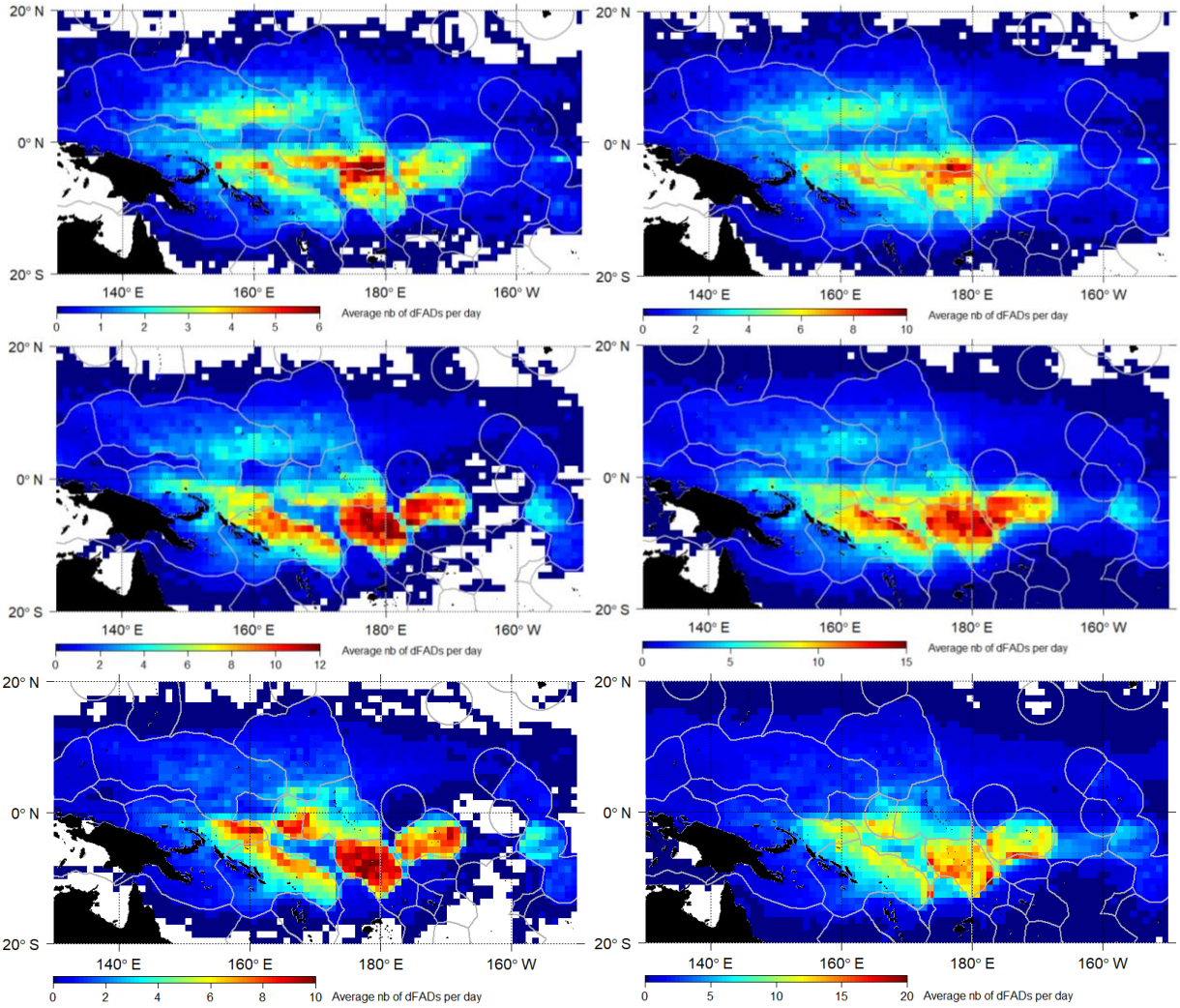

Figure 19. Observed (left) and corrected (right) density of the average number (nb) of FAD satellite buoys transmitting at least once per day and per 1° grid cell during 2016 (top), 2017 (middle) and 2018 (bottom).

5.3. Impact on CPUE

The influence of FAD density on CPUE, catch per set, and the occurrence of FAD and free school sets was investigated using the corrected FAD densities described above combined with aggregated and corrected logsheet data ("S-BEST") per 1° grid cell and month or operational data from observer records at the set level (Table 3; Figure 20).

The "S-BEST" logsheet data corresponds to the most complete dataset corrected for species composition aggregated by 1° cell and month. However, in order to access the catch per set and add

additional variables to the models, we also used observer data. By matching set position and date in observer data and FAD trajectory in the PNA FAD tracking data (Escalle et al., 2018b), we accessed the drift duration of each FAD that was set on, as well as if the attached satellite buoy had an echo-sounder (based on the model and brand types derived from the buoy ID format). In addition, we also selected sets with FAD characteristics recorded by the observer (i.e., depth of submerged appendages, length and width, origin of the FAD). Finally, we compiled lunar phase and thermocline depth data (i.e. isocline 15°C from ECMWF Ocean reanalysis System 4).

Generalised additive models (GAMs) were used to assess the influence of FAD densities and other variables on catch per species, CPUE, and number of associated and unassociated sets. Model selection was performed using a backward stepwise selection procedure based on model selection criteria (Akaike's Information Criterion (AIC), Bayesian information Criterion (BIC)), residual analysis, examination of predicted versus observed values, and deviance explained. Note that models per area and/or year were tested and showed similar results.

Table 3. Number of associated (Ass.; i.e. FAD and log) and unassociated (Unass.) sets recorded in aggregated "S-BEST" logsheet and in the observer datasets and used in the models to evaluate the influence of FAD density on CPUE and catch per set.

		Aggregated S-Best logsheet data	Observer data	Observer data matched with a FAD trajectory	Observer data matched with a FAD trajectory and with FAD characteristics
2016	Ass.	12,776	9,758	2,765	418
	Unass.	31,686	21,404		
2017	Ass.	15,846	8,008	2,380	286
	Unass.	33,024	15,813		
2018	Ass.	17,457	9,397	2,561	368
	Unass.	32,972	16,428		

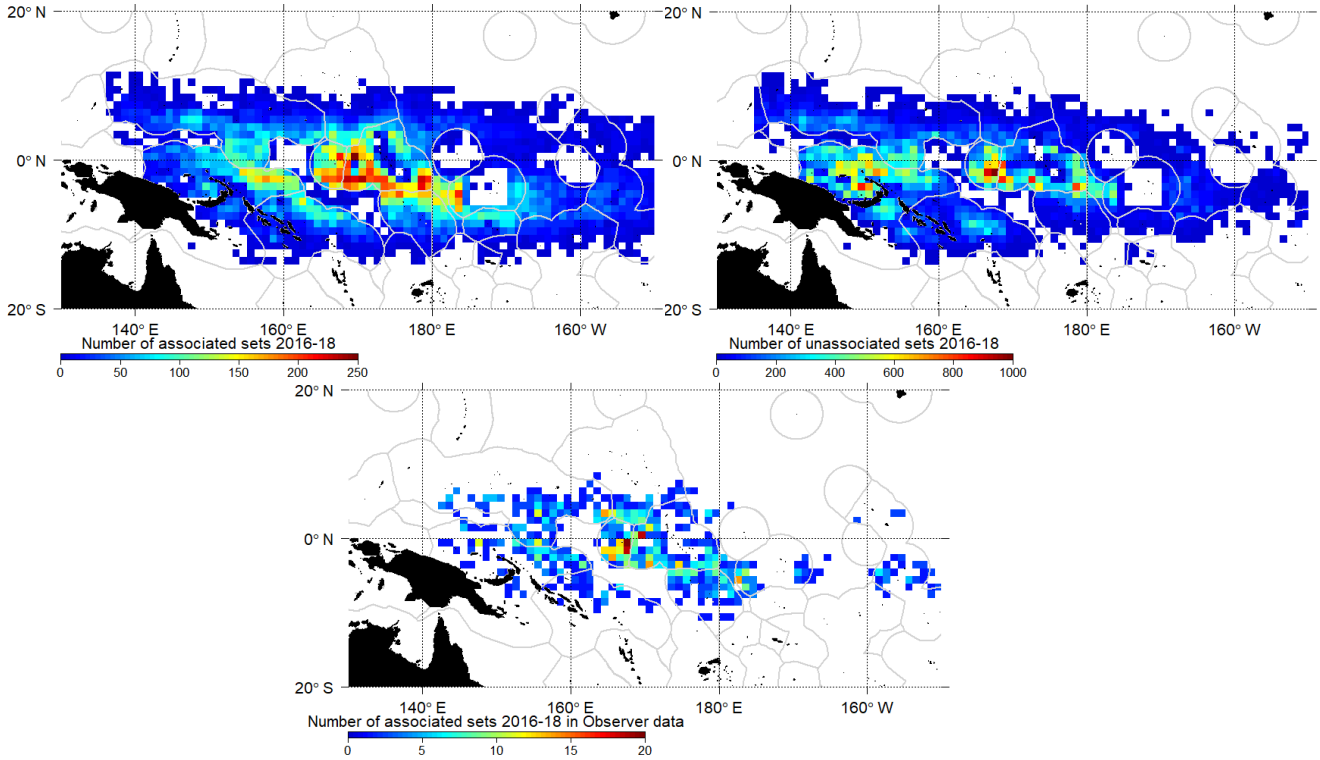

Figure 20. Spatial distribution of the 2016–2018 associated and unassociated sets from S-BEST logsheet aggregated data (top) and from observer data (bottom; sets with FAD characteristics recorded and that have been matched with a FAD trajectory in the PNA FAD tracking data) used in the GAM models. Note the difference in colour scaling between figures.

5.3.1 Monthly corrected FAD densities and logsheet CPUE

Two sets of GAM models were performed to evaluate the influence of FAD densities on the occurrence of associated and unassociated sets, as well as related CPUE (catch/ number of sets) per species on a monthly basis (Table 4). Corrected FAD densities; 1° cell latitude and longitude; Southern Oscillation Index (SOI; proxy for the ENSO cycle); and one first-degree interaction term between variables were used as explanatory variables. CPUE per species, total CPUE, and number of sets were the response variables in each model. Models explained 5 to 27.2% of total deviance and all variables were significant except SOI in models of set occurrence and several of the unassociated CPUE GAM models (Table 4).

First, regarding the first set of models on associated set occurrence and CPUE, an increase in the number of associated sets was detected with increasing FAD density (Figure 21), which was expected given that the highest FAD densities occur in the main FAD fishing areas (Figure 20). A slight decrease in CPUE with increasing FAD density was detected for skipjack, bigeye, and total CPUE (Figure 21). In particular, for skipjack CPUE, apart from a decrease for very low FAD densities (<30 per 1° cell), CPUE increased until approximately 180 FADs were present at least once per 1° cell and per month, then it decreased. Note that Escalle et al. (2018a), found that FAD densities corresponded to an index accounting for the number of FADs in a 1° cell and the time spent in it, while FAD densities considered here correspond the overall number of unique FADs transmitting and simulated per 1° cell per month.

Secondly, the number of unassociated sets increased with low FAD densities (0 to 50 FADs per 1° cell per month), then remained stable, or increased with very high FAD densities (Figure 21). CPUE by species and total unassociated CPUE both decreased with increasing FAD density.

FAD density was also found to affect the presence of bigeye tuna during the pre-dawn period, time of FAD purse seine setting (Joe Scutt Phillips et al., 2019), with higher likelihood of association with the FAD at that time when the daily FAD density is high. In this study a decrease in bigeye CPUE was detected with increasing monthly FAD density, at least for the low levels of FAD density, then the CPUE was stable. It appears that there might be contrasting effects of FAD density on bigeye tuna at different spatio-temporal scales, between monthly CPUE and density data, to daily presence at a given FAD and daily density. This should be examined further.

Table 4. Log-normal GAM models in the WCPO using aggregated logsheet data from 2016-2018 combined with a list of significant variables, percentage of deviance explained, and pseudo coefficient of determination (R^2).

Models		Significant explanatory variables	Deviance explained	R^2
Associated set	Number of sets	LAT, LON, FAD density, ti(FAD density, LAT)	18.5	0.18
	BET CPUE	LAT, LON, FAD density, SOI, ti(LAT, LON)	27.2	0.27
	SKJ CPUE	LAT, LON, FAD density, SOI, ti(LAT, LON)	8.3	0.08
	YFT CPUE	LAT, LON, FAD density, SOI, ti(LAT, LON)	8.9	0.09
	Tot CPUE	LAT, LON, FAD density, SOI, ti(LAT, LON)	6.7	0.07
Unassociated set	Number of sets	LAT, LON, FAD density, ti(FAD density, LAT)	8.2	0.08
	BET CPUE	LON, FAD density, ti(FAD density, LON)	8.1	0.08
	SKJ CPUE	LAT, LON, FAD density, SOI, ti(LAT, LON)	5.5	0.05
	YFT CPUE	LAT, LON, FAD density, ti(FAD density, LAT)	12.8	0.13
	Tot CPUE	LAT, LON, FAD density, ti(FAD density, LAT)	1.4	0.01

ti = first-degree interaction term between variables

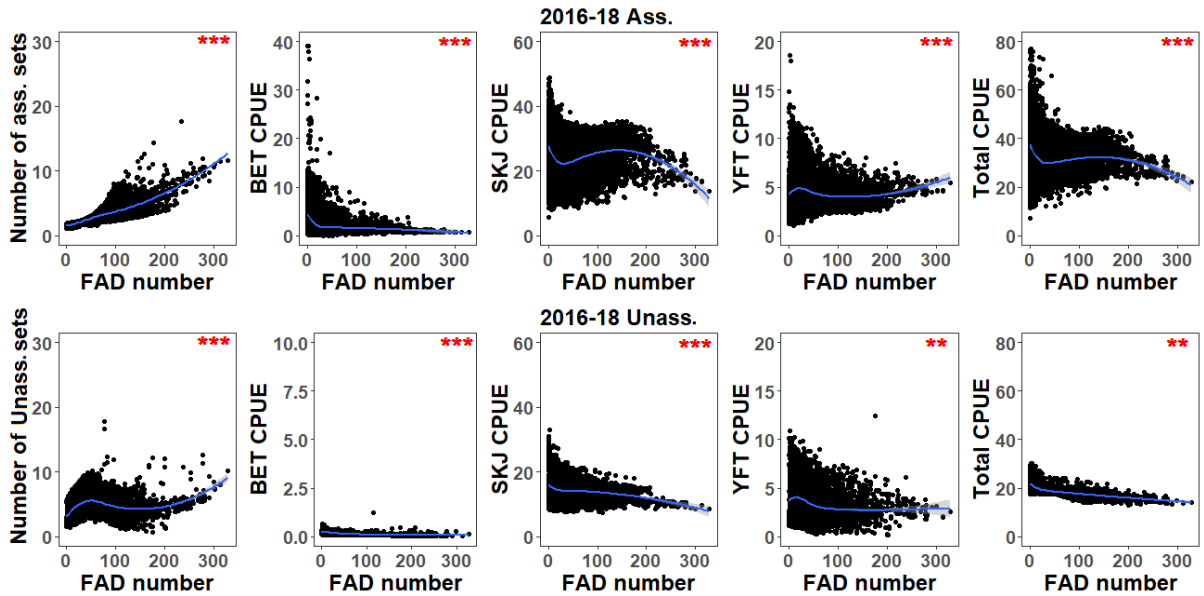

Figure 21. Associated (top) and unassociated (bottom) number of sets, and CPUE per species as a function of the number of FADs per 1° cell and month, as fitted by the GAM models. The blue line is the smoothing regression (loess) with grey shaded region representing the 95% confidence interval. Red stars indicate the significance of each variable in the models.

5.3.2 Daily corrected FAD densities and observer catch per set

The influence of daily FAD densities on the catch per set from observer data was also evaluated, to account for environmental variables and characteristics of the FAD set on. A total of 7,706 sets from the observer dataset were matched with a FAD trajectory, of which 1,072 included FAD characteristics. Drifting durations were estimated from the PNA FAD tracking data, but corresponded to the buoy drift duration, not necessarily the FAD drift duration, if the buoy had been deployed on an already drifting FAD. In addition, it did not account for potential sets that may have occurred in the lifetime of the FAD before the current considered set. Therefore, this variable should be considered here with caution, and additional processing would be needed before accessing real FADs drifting durations, at least for a subset of the FAD sets. For these reasons, sets on FADs with an estimated drifting duration of less than five days were removed, as they were considered unlikely to correspond to the true FAD drifting duration. Models therefore only included 521 sets and the corresponding catch, with all variables available.

Explanatory variables tested included corrected FAD densities; latitude; longitude, SOI; drift duration; moon phase; thermocline depth; FAD depth; FAD size (length*width); and the presence of an echo-sounder and origin of the FAD as factors. Response variables were bigeye, skipjack, yellowfin, or total catch per set. Models explained 7.4 to 20% of total deviance (Table 5). Thermocline depth, FAD size, and the origin of the FAD were not significant in any of the models.

Table 5. Log-normal GAM models in the WCPO using observer data from 2016-2018 combined with a list of significant variables, percentage of deviance explained, and pseudo coefficient of determination (R^2).

Models	Significant explanatory variables	Deviance explained	R^2
BET catch	Lat, FAD density, Moon, echo sounder	20.0	0.17
SKJ catch	Lon, SOI, FAD Depth, Drift duration	12.6	0.11
YFT catch	Lat, FAD density, SOI	11.7	0.10
Total catch	Lon, SOI, FAD Depth, Drift duration	7.4	0.06

While FAD density was a significant variable in the aggregated CPUE models, it was not significant in these models of skipjack catch per set. However, skipjack catch increased with drift duration (Figure 22). Specifically, a sharp increase was detected with short drift duration, with continued but smaller increases with durations over 30 days. FAD depth, as recorded by observers, also influenced skipjack catch, with high catches on FADs with submerged appendages of approximately 30m or deeper than 70m. However, the uncertainty with the way observers collect this information (raw estimates, especially when the FAD is not lifted) should be kept in mind. FAD densities were significant in the models of bigeye and yellowfin catch per set, with a decrease in catch per set with increasing FAD densities. Moon phase was only significant in the bigeye catch model, with higher bigeye catch in the last quarter. Of note is that lunar illumination was also a significant term in models explaining bigeye presence at FADs during pre-dawn setting period in recent electronic tagging study (Joe Scutt Phillips et al., 2019). It showed increased presence at quarter and full moon periods. Finally, SOI was significant in all the models, except bigeye catch, highlighting ENSO influence and the inter-annual variability, although the 2016-2018 period generally did not display high ENSO variability.

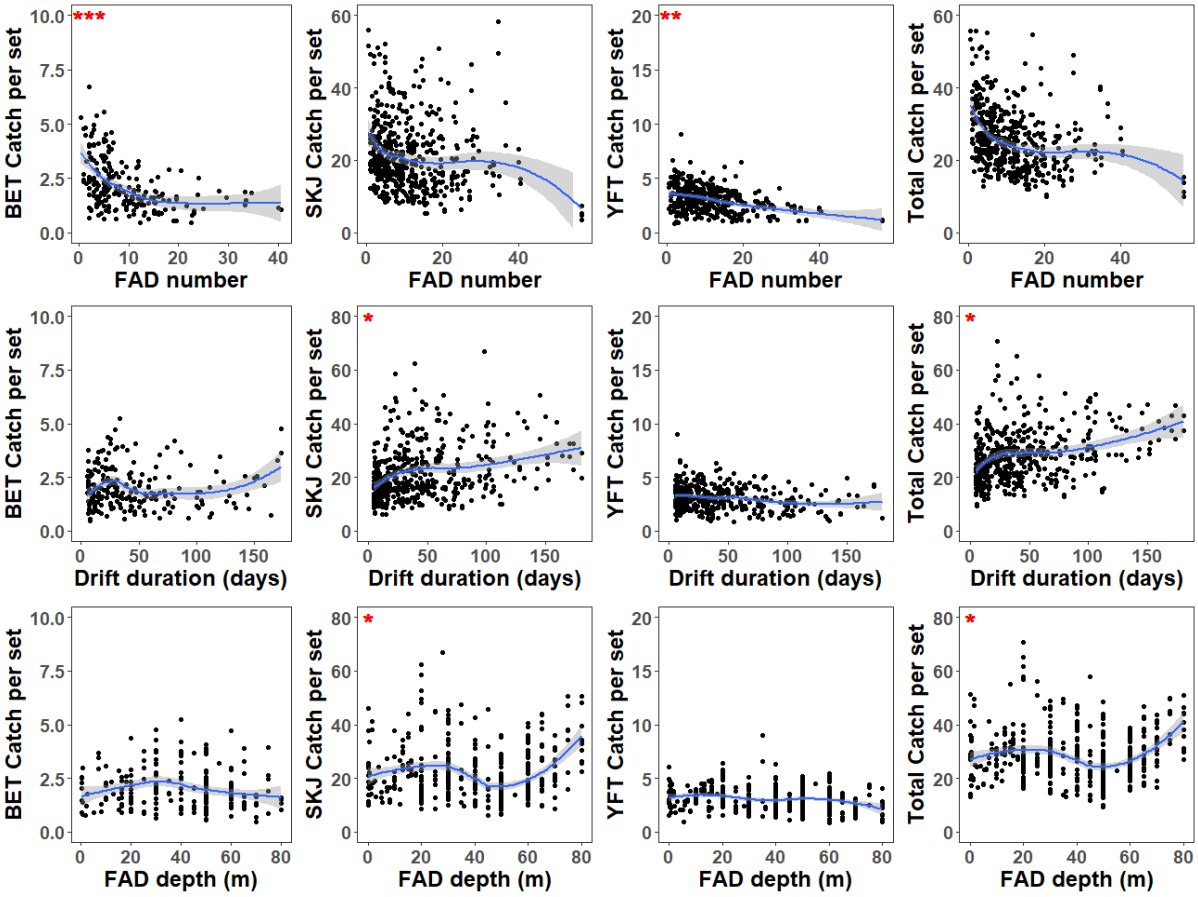

Figure 22. Relationships between catch per species on associated sets and FAD densities (top); FAD drifting duration (bottom), and FAD depth (bottom), as fitted by the GAM models. The blue line is the smoothing regression (loess) with grey region representing the 95% confidence interval. Red stars indicate the significance of each variable in the models.

5.4. FAD network

Relative FAD density indices could also be compiled when considering the total number of FADs drifting at sea (uncorrected data, i.e. from the PNA FDA tracking dataset), as a network, and investigating the inter-FAD distances and the probability of a vessel randomly encountering a FAD within this network.

Given the extended computation time to calculate daily inter-FAD distances, we investigated only a single month in 2018 (February, when the transmission frequency was relatively consistent with previous months). We randomly selected the date of February 20th 2018 to compile the inter-FAD distances (see Figure 24 for the general position of the FADs on that day). The distance between each drifting FAD to the next closest drifting FAD was calculated and investigated by EEZ (Figure 23). The distribution of inter-FAD distances varied depending on the EEZ, and reflected patterns found in the FAD density distribution (Figure 14). In the Federated States of Micronesia (FSM) and the Marshall Islands' EEZ, the inter-FAD distances were generally higher than in the other EEZs and varied from less than 10km to 100km (Figure 23). While very large distances were also found in PNG, the core of the distribution is 20–30km. In the Tuvalu EEZ, which had the highest FAD density, FADs were 7–18km apart, with a large peak for inter-FAD distances of less than 10km.

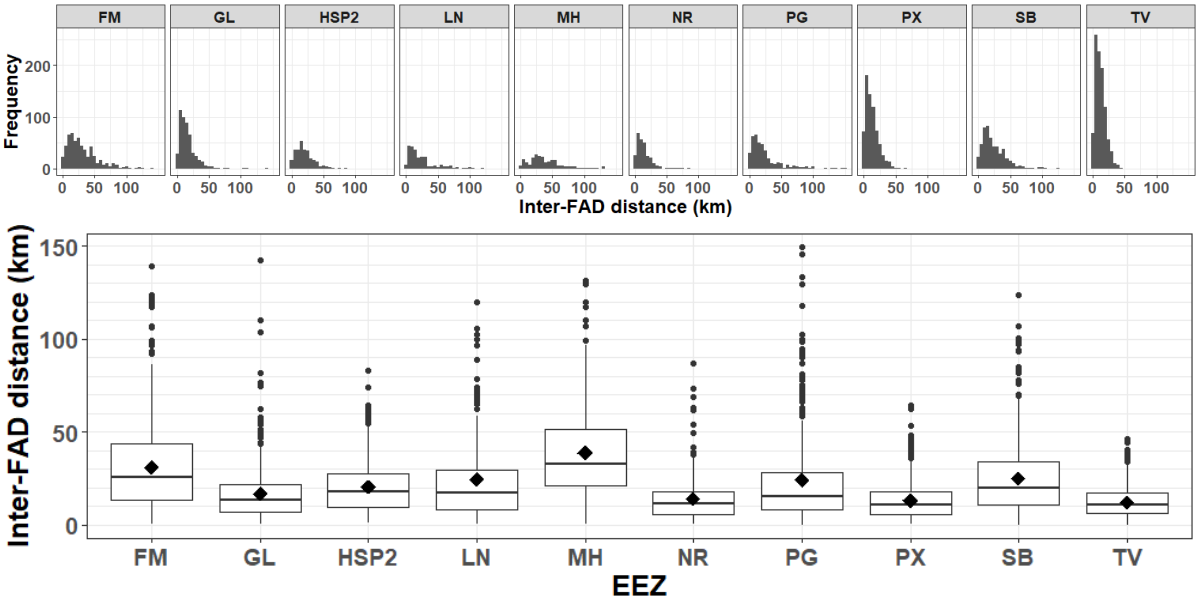

Figure 23. Histogram and boxplot of the minimum distance between each individual FADs drifting in the WCPO, by EEZ, on February 20th 2018. EEZs with less than 50 FADs were removed.

To complement this exploratory analysis, we considered three hypothetical trips: Pohnpei-Tarawa; Honiara-Funafuti; and Port Moresby-Majuro, and looked at the number of days in February 2018 where at least one FAD was less than a certain distance from the vessel track (0.5–10[1] nautical miles (nm), see Figure 24 and Table 5). It was found that every day of the trip at least one FAD was found at less than 2nm (10nm for Pohnpei-Tarawa) of the trips (Table 5). The Pohnpei – Tarawa trip, where the FAD density is relatively low, had 32.1% of days with at least one FAD within 0.5 nm. The Port Moresby–Majuro and Honiara-Funafuti trips, which cross areas of very high FAD densities, had high rates of predicted encounters (78.6 and 92.9% respectively). Therefore, there is a high probability of a vessel encountering a FAD randomly. It can, nevertheless, be noted that even for those trips in February, some areas appear to generally have few FADs, decreasing the chance of randomly finding one, although this may vary temporally.

Table 5. Percentage of days with FADs found within 0.5–10nm of three imaginary trips in February 2018.

Distance in nautical miles	≤ 10 nm	≤ 2 nm	≤ 1 nm	≤ 0.5 nm
Pohnpei - Tarawa	100.0%	96.4%	67.9%	32.1%
Honiara - Funafuti	100.0%	100.0%	96.4%	92.9%
Port Moresby - Majuro	100.0%	100.0%	89.3%	78.6%

[1] 10 nautical miles would be the average maximum distance traveled by a vessel in one hour, given a cruising speed of 10 knots.

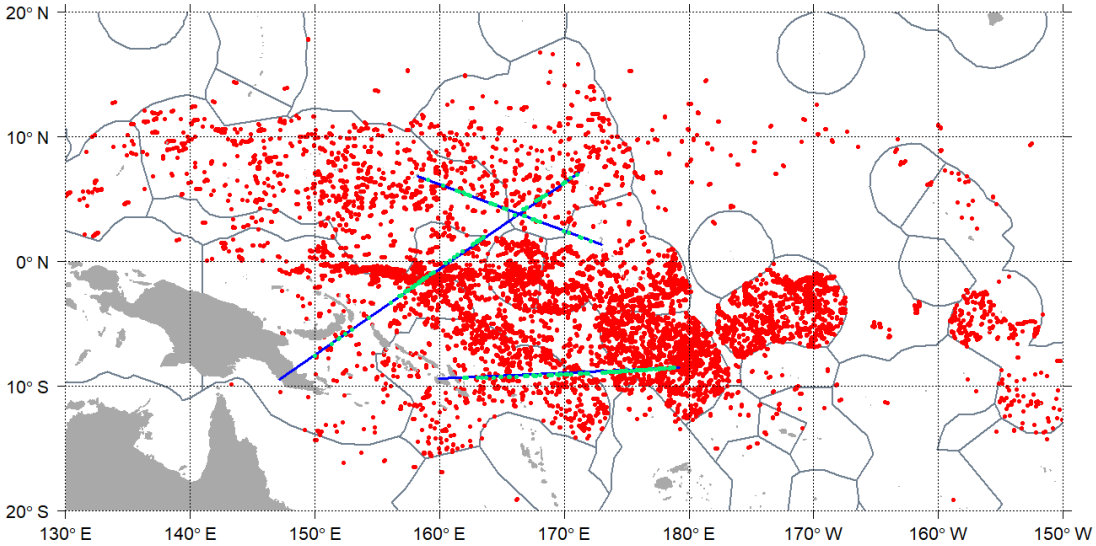

Figure 24. Distribution of FADs on the February 20th 2018 (red dots), with three imaginary trips (blue lines), and the FADs found at less than 1nm of these lines for at least one day during February (green dots).

6. Matching with VMS data

An attempt was made to match vessel positions from VMS data with FAD tracking data. This could be used to: i) validate deployment position and access FAD characteristics linked to the deployment; ii) link associated fishing set with the corresponding FAD; iii) detect FAD fishing activities (deployment, set, visit) during the FAD closure; and iv) follow the life history of a specific FAD through appropriation and leasing processes.

Five vessels with available FAD tracking data were randomly selected to test this methodology. Each VMS position from these vessels (during fishing, transiting, and in-port) from January to September 2018 were matched with the FAD tracking data based on position and date/time. First, transmissions from buoys at a maximum distance of 27.8 km from a VMS position and 1h before or after that VMS transmission were selected (considering the variability in buoy transmissions (from every hour to every day) and vessel maximum speed of 15 knots = 27.8 km/h; Figure 25).

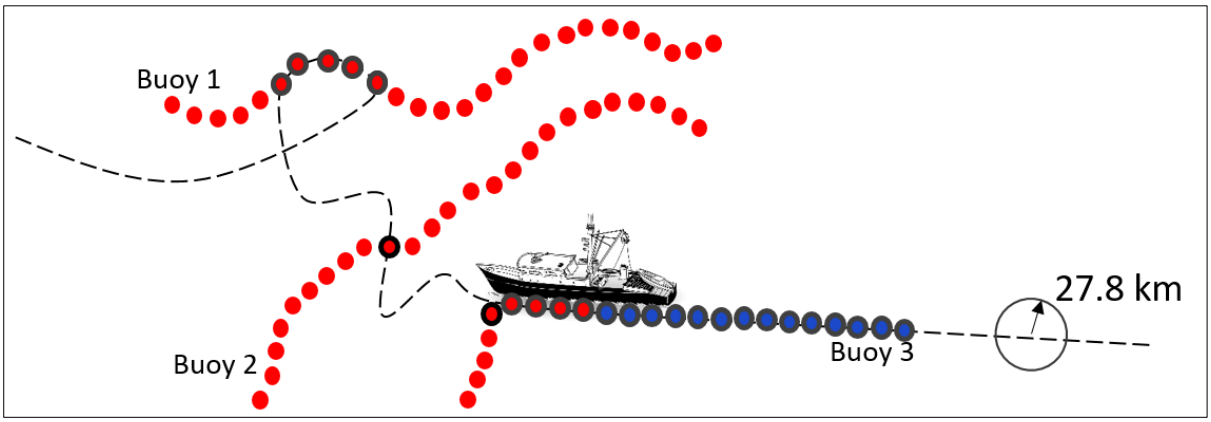

Figure 25. Diagram of VMS and FAD tracking data matching based on position (distance ≤ 27.8 km) and date/time (time ≤ 1 hour). The dashed line represents the VMS track; red and blue dots represent the at-sea (red) and on-board (blue) FAD transmissions, those with a black edge denote when FADs were matched with the VMS track.

While it is possible that a FAD could be, at random, less than 27.8 km from a vessel in a 1h period but not seen by it (see following section), it is important to identity the actual visit of a vessel to a FAD. We defined matching as the close association in space and time between a FAD transmission and a vessel VMS transmission, which may be different from the visit to the FAD (set, deployment, service it). This is particularly true in our data, given the fact that both VMS and FAD buoys mostly transmit every hour, but not at exactly the same time. A similar matching has been previously performed using associated set in logsheet data in the same way (Escalle et al., 2017b, 2018b). The proportion of FAD sets from the logsheet data that could be associated with a particular buoy in the FAD tracking database was then used as an estimate of the coverage rate (30–40%) of the FAD tracking data.

To investigate patterns of vessel-FAD distance (where distance <27.8km), matching events were separated into different vessel activity categories (based on the VMS track classification): i) vessel in port; ii) vessel in fishing activity (matched with own FAD on-board; matched with own FAD at sea; or matched with FAD from another vessel at sea); and iii) vessel transiting (Figure 26). Note that buoys may be on-board a vessel, drifting at sea and visited by the vessel, or drifting at sea but not visited by the considered vessel (e.g. owned by another vessel). FAD positions matching vessels in port were mostly identified to be less than 5 km from each other (Figure 26c). Similar results were found for vessels in fishing activity, with most matched FADs found less than 5 km from the vessel, indicating a likely FAD visit by the vessel (Figure 26a). Finally, a completely different pattern was found for transiting vessels, with a wide range of FAD-vessel distances (Figure 26b), potentially indicating that some FADs may come relatively close to a vessel but were not visited; or simply linked to the higher cruising speed of vessels when transiting. However, this specific pattern was found for transiting vessels matched with a buoy on-board the vessel owning it. We are therefore confident that all distances in the 0–27 km range could represent an actual visit to a FAD.

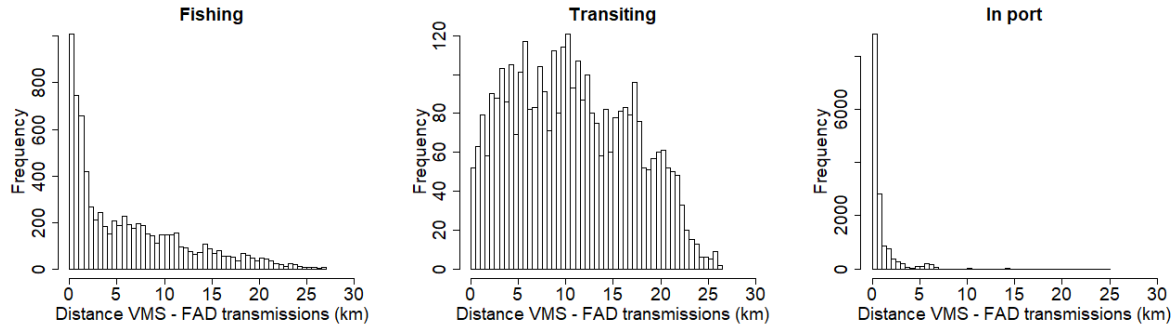

Figure 26. Histograms of the distance between a vessel and a FAD position separated by 1h maximum. Note the difference in y-axis scale.

The number of matching VMS and FAD positions between a specific FAD and a vessel was also considered to indicate a visit to a FAD (Figure 27). We focus on the January to June period to investigate patterns FAD use is normal (outside the closure). When matching with vessels undertaking fishing activity (setting, deploying, searching for tuna schools, etc.; as classified based on VMS track patterns), most FADs belonging to the vessel and drifting at-sea were matched to the vessel for 5–50 buoy transmissions, compared to 2–16 for FADs of the company and 1–8 for other vessels' FADs (Figure 27). This means that when owned by the nearby vessel, there were more consecutive buoy transmissions matched with the VMS than for the other groups. For transiting vessels, few FADs were matched to a vessel for more than nine transmissions. Similar trends were found for on-board FADs, although a very wide distribution was found for FADs of another vessel of the same fishing company

(Figure 27). Generally, when looking at matching events between vessels fishing and their own FADs, 78% and 64% of at-sea and on-board FADs had more than five transmissions matched with the VMS transmissions (up to 88% and 75% for more than three transmission matched). Therefore, we defined a visit as a match between a FAD and a vessel, with more than five buoy transmissions matched with VMS transmissions. It can be noted that for FADs with a low transmission frequency (>1 per hour), visits may be underestimated.

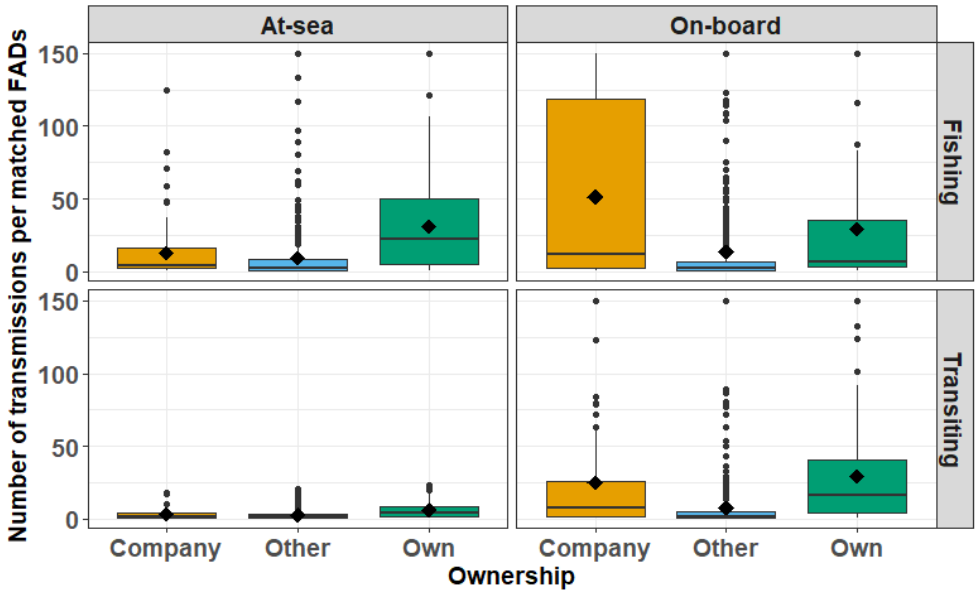

Figure 27. Number of transmissions for FADs matched with a vessel depending on the ownership of the FAD, its state (at-sea vs on-board), and the vessel activity.

7. Fate of FADs

7.1 General classification

Buoy positions at the end of their trajectories were investigated to study the fate of FADs. The end of a trajectory was classified as: i) still drifting if the last position was "at-sea" and within the main purse seine fishing grounds (141°W, 210°E, 8°N, 12°S); ii) lost if the last position was "at-sea" but outside the main purse seine fishing grounds or at a PNA member EEZ border; iii) recovered if the last position was "on-board"; or iv) beached. Beaching events were identified as a FAD having i) the last position "at-sea" and within 10 km of shore (excluding positions located at less than 10km from major ports); and ii) at least the last three positions at 0m, <10m, or <100m from each other. This was based on data from 2016 to 2018. To remove potential bias in the analysis due to buoys that might transmit again when data are loaded again in the near future, buoys with transmissions over the last 8 months of the dataset (April–November 2018) were removed.

The majority of FADs (58.3%) were still drifting within the main purse seine fishing grounds at the time of their last transmission (Figures 28 and 29). Further investigation revealed that 10.1 and 7.7% of the FADs had their last transmission in December or during the FAD closure, two periods when FADs are deactivated in high numbers (Figure 9). This will lead to the presence of unmonitored FADs drifting in the fishing grounds, increasing the number and density of active FADs on the fishing grounds that are not captured in the analyses described above. In addition, 8.6% of FADs were at the edge of the main

fishing grounds (within an area comprising the two exterior 1° squares surrounding the main fishing grounds at the time of signal loss; Figure 29a), and 9.0% were 50 km from shore, indicating potential loss or beaching in the near future. However, this should be interpreted carefully given that local currents can bring FADs back to the fishing grounds or away from shore.

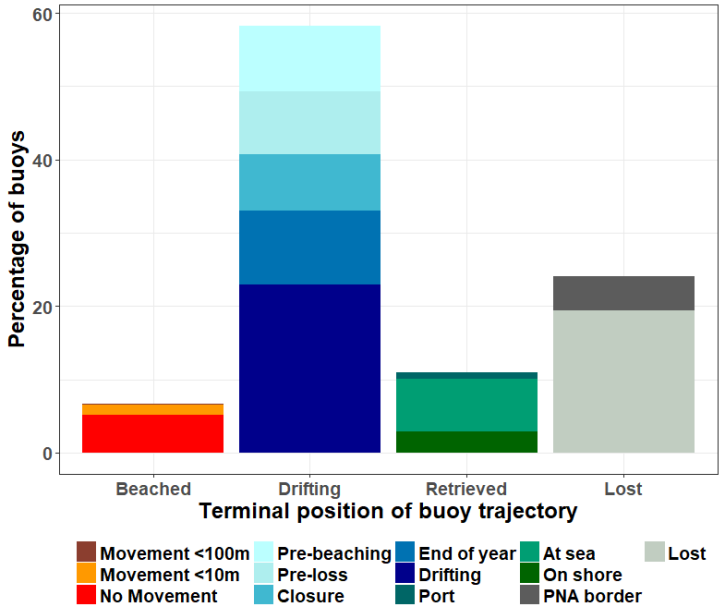

Figure 28. Percentage of buoys' terminal position classified as beached; drifting; retrieved by any vessel; or lost in 2016–2018 period.

The remaining FADs were either found to be lost (24.0%), i.e. drifting outside the main purse seine fishing grounds or bordering a PNA EEZ and the high seas, or retrieved (10.1%), i.e. with their last position classified as on-board a vessel (Figures 28 and 29). However, there is no indication whether the vessel retrieving the FAD was that owning the FAD, another purse seine vessel, or another vessel (for example when the recovery is close to shore). In addition the map of recovered FADs in Figure 29 corresponds to the last position of the recovered FADs, which could be in a port, while it would be relevant to map the first position post-recovery of these FADs. Finally, 6.7% of the FADs were beached, with most (5.2%) not moving at all at the end of their trajectories (Figures 28 and 29).

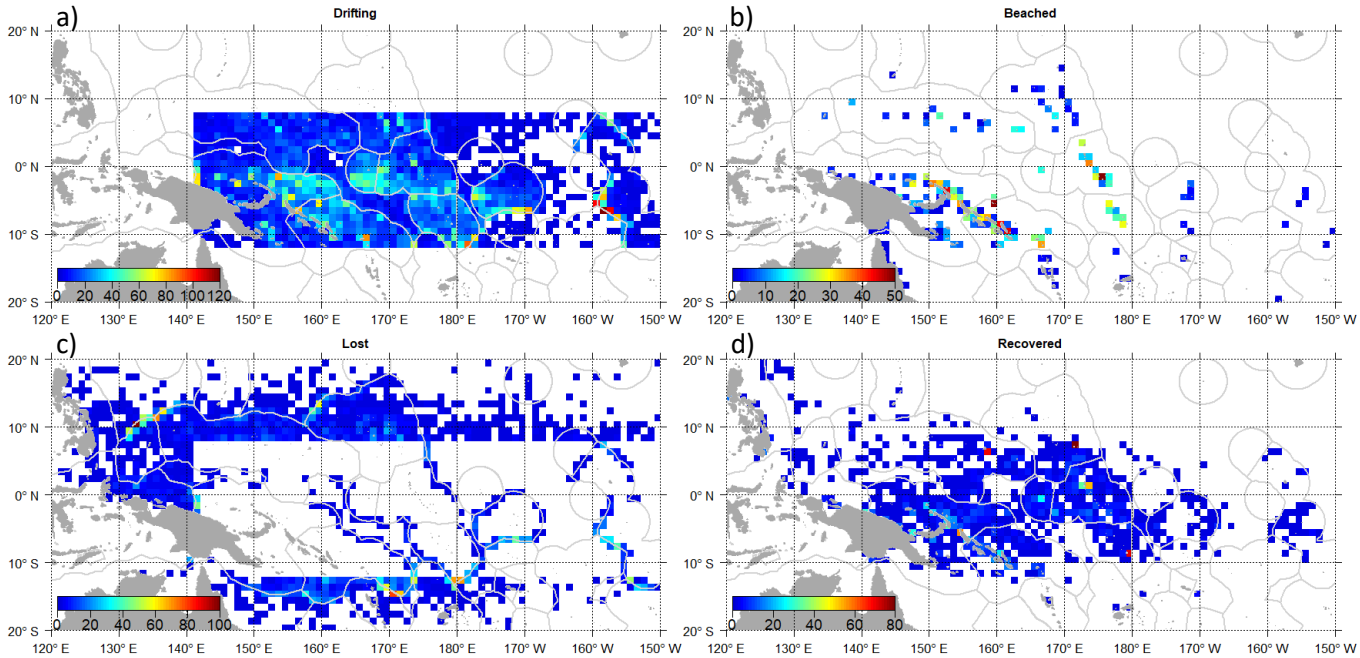

Figure 29. Density maps of last recorded position of each buoy in the FAD tracking data: a) still drifting; b) beached; c) lost; and d) retrieved in 2016–2018 period.

7.2. Distance from companies' fishing grounds

To refine this general classification and better identify lost FADs, the distance between the last position of a FAD and the fishing ground of the company owning it was assessed. This has the potential to better indicate the potential for a fleet to recover FADs that would become 'lost', based upon current practices. The distance between the last position of a FAD and either the edge of the core (0.99 quantile of number of purse seine sets per 1° cells) and extended (0.90 quantile) fishing grounds (all purse seine sets) of the company were calculated. Only companies with at least three purse seiners were considered. The distance of the FAD from the nearest port was also examined, to identify whether recovery from that location was feasible.

Figure 30 shows the fishing grounds of some fishing companies during a given year, with an example FAD track from the related company.

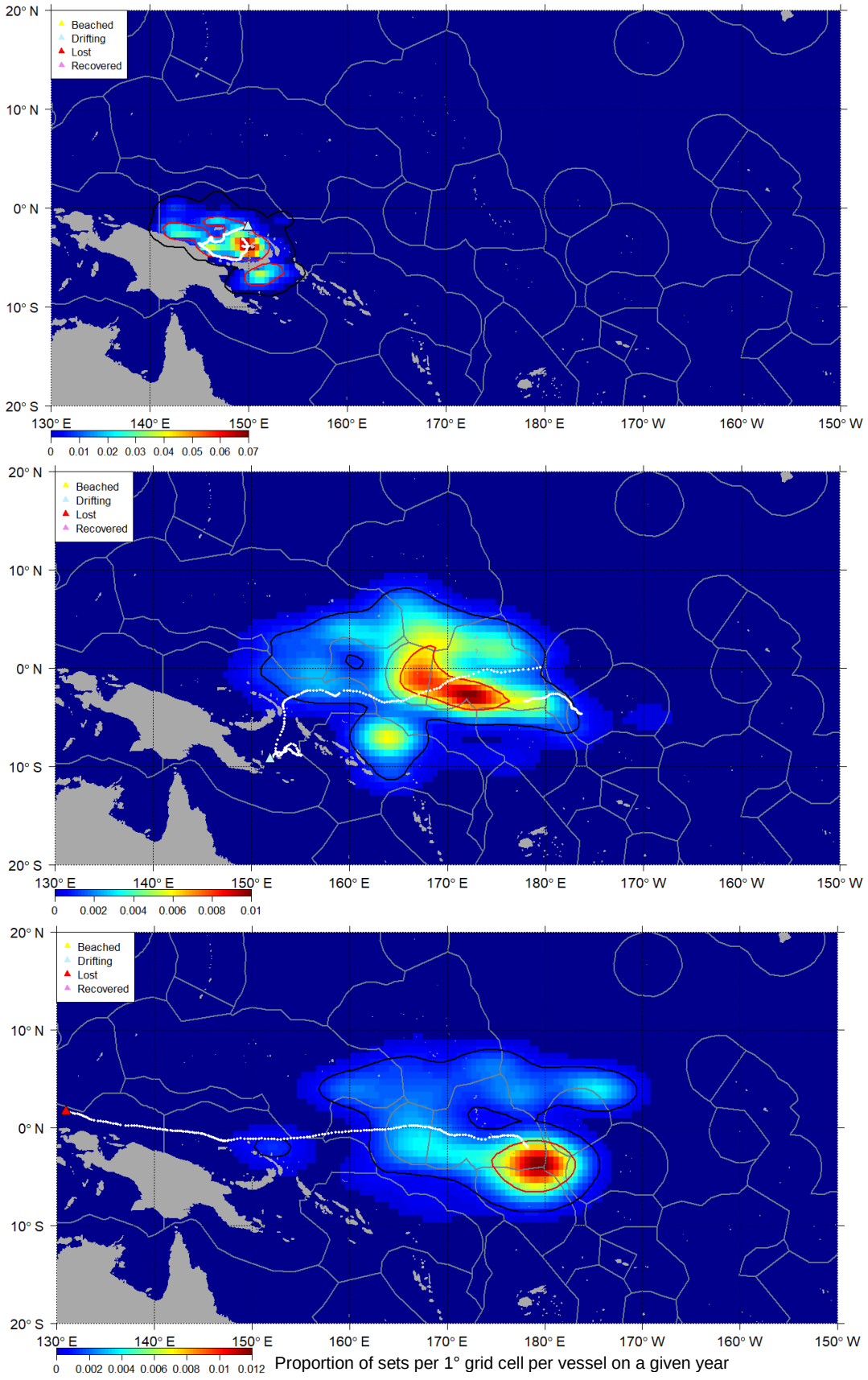

Figure 30. Density map of purse seine fishing sets of three different fishing companies in 2016 or 2017, with the track of a FAD from that company depicted in white. Black and red lines correspond to the extended (0.99 quantile) and core (0.90 quantile) fishing grounds.

The distribution of the distance between the last position of lost FADs and core fishing ground of the company owning the FAD was of 1,000–2,700 km, with an average of 2,000 km (Figure 31). When considering the extended fishing ground it decreases to 300–1,600 km, with an average of 1,000 km. Finally, lost FADs were found at a distance of 500–900 km from port, with an average of 750 km.

For the FADs found beached, recovered, or still drifting at the end of their trajectories, the distances from core and extended fishing grounds were shorter, with averages around 1,000 km and 300 km, respectively (Figure 31).

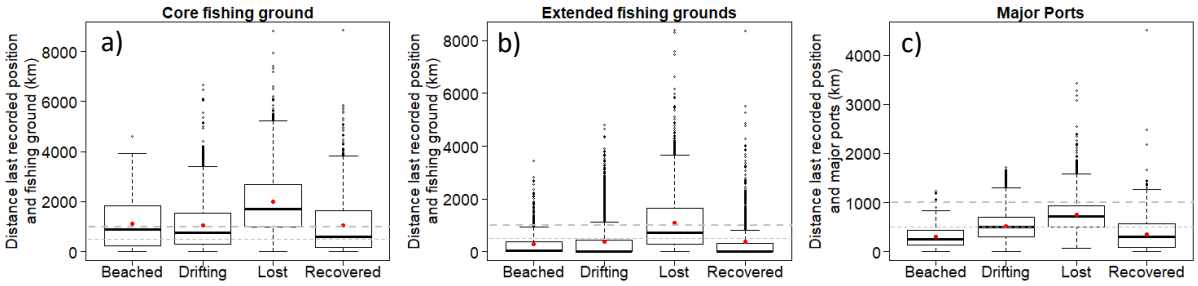

Figure 31. Distance between the last recorded position and the a) core fishing ground of the company owning the FADs; b) extended fishing grounds; c) closest major port, depending on the general classification of FAD fates described above. Dotted grey lines indicate 500 and 1000 km.

7.3. Reclassification using distance from companies' fishing grounds

The classification of a "lost" FAD was re-assessed, taking into account the fact that the last position was outside the extended fishing ground of the company owning the FAD, rather than the general purse seine associated fishing ground (Figure 32). Under this classification, the majority of FADs were lost (51.8%), with 29.5% being found within the fishing grounds of all purse seiners, and 22.3% outside the main fishing grounds. At the same time, the number of FADs classified as still drifting at the end of their trajectory decreased to 29.4%, half being FADs deactivated at a specific time (end of the year or during the closure) or with transmissions not transferred to the PNA (i.e. the last position at the border of a PNA member EEZ).

We may hypothesise that FADs found drifting within the main purse seine fishing grounds with unexplained deactivation (classified as "drifting" and "pre-beaching" in Figure 32) correspond to FADs that have sunk, buoys being disabled during FAD appropriation by another vessel, or buoy malfunction. Except for in the latter case, the remaining categories would not lead to FADs floating unmonitored. Lost FADs would remain in the water for an unknown period of time, and this number of unmonitored FADs should be taken into account when assessing FADs densities, and when reviewing the impact of FAD density on CPUE.

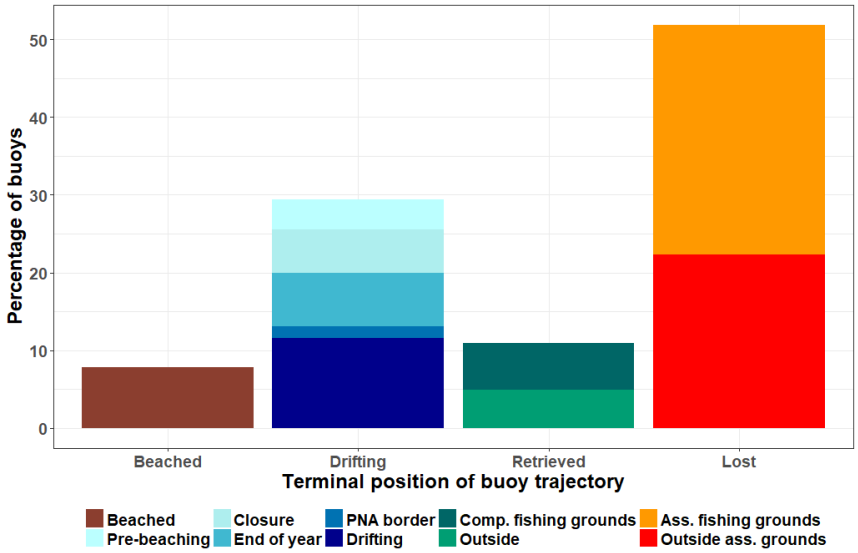

Figure 32. Percentage of buoys' terminal position classified as beached; drifting; retrieved (within or outside the fishing grounds of the company owning the FAD) by any vessel; or lost (within or outside the general purse seine associated fishing grounds, i.e. see Figure 29) from 2016–2018. These results are based on FADs from companies with at least three purse seiners and with the last transmission in the dataset before July 2018 (12,315 FADs).

In summary, using this refined approach to classify the fate of a FAD, we estimated that 51.8% of FADs were lost; 10.1% were retrieved; 6.7% were beached; 14.0% were deactivated by the fishing company and left drifting unmonitored at sea; and 15.4% were sunk, stolen, or with a malfunctioning buoy. Overall, if we included those deactivated FADs and the ones lost but still within the purse seine fishing grounds, we estimated that 5,359 FADs (43.5%) are unmonitored within PNA waters. In turn, distances between FADs and the 'owning' fleet are significant, and may hinder direct recovery.

8. Discussion and Conclusion

The data volume submitted to PNA has clearly increased overtime, and quality of the data for analysis can be improved through the implementation of the filtering and processing methods undertaken here. However, the lack of full submission of the data by fishing companies and the editing of the data before submission to PNA, limits and complicates the analyses and outputs of potential interest for management purposes. However, a simulation procedure based on ocean currents was implemented to correct FAD densities, which greatly improved the estimation of FAD numbers per day and the spatial distribution of FAD densities. Note that FADs not appearing in any PNA EEZ (high seas or other EEZs only) are likely to be rare, but would not be seen at all in this data set. Additional parameterisation of the simulation method is still needed, and various ocean current models could be tested and compared. Similarly, it would be relevant to simulate the drift trajectory of FADs with a known and complete FAD trajectory, to quantify the accuracy of simulated tracks at different spatial resolutions. Nevertheless, complete and unmodified FAD tracking data will always remain the most precise source of information regarding FAD densities and number of FADs or buoys at-sea.

Where these tracking data are currently most complete, within PNA EEZs, this paper has revealed the degree to which density and inter-FAD distances vary. In PNA countries such as Tuvalu, where almost half of all FADs are less than 10km from each other, this may have significant effects on the behaviour and vulnerability of tropical tunas. The direct effect of FADs on these species is believed to occur at

around this distance (Moreno et al., 2007), with directed movements towards FAD-aggregated schools identified from 10km away in electronic tagging studies (Girard et al., 2004). Similarly, extensive but continuous associations between two close FADs by bigeye and yellowfin tuna have been observed in recent sonic tagging studies in the WCPO (Joe Scutt Phillips et al., 2019). Given the very close distance between the majority of FADs in EEZs such as Tuvalu, the possibility that any school does not 'associate' with a FAD during any given 24-hour period must be considered. Catch and tagging data that exist within these networks of short inter-FAD distances could be examined to further quantify the likely effect on free schooling and associated behaviours within these FAD dense, but data-rich, areas.

The importance of *in-situ* data related to FAD characteristics (observer data as recorded until now or captain's records) has also been highlighted. In particular, FAD depth and FAD drift duration have been shown to influence catch per set. Hence, we emphasize again the need for precise records of i) manufacturer buoy ID number; ii) FAD and buoy deployment date (given that FADs themselves are marked); and iii) information on the FAD (depth, width/length).

A new method based on the distance between last transmitted position of a FAD and the main fishing ground of the company owning, enabled better estimates of FAD fates. In particular, it highlighted the high rate of FAD loss (>50%) and FAD beaching (7 %). However, it is clear that the lack of complete FAD trajectories underestimates the number of beaching events, specifically in non-PNA countries. In addition, even with a complete FAD tracking dataset, buoys may be deactivated before reaching coastlines, leading to unnoticed beaching events. This therefore highlights the importance of considering the use of bio-degradable FADs in the WCPO, and/or potentially considering buoy recovery programs or more collaboration between fishing companies when buoys drift out of one company's fishing grounds to mitigate impacts.

Potential additional research topics include:

- Additional work and parametrisation of the simulation method to re-construct FAD tracks with missing sections. For instance, different current models could be tested, but also validation of the different ocean forcing models using known trajectories is needed.
- Further investigate the link between FAD densities and occurrence of FAD and free school sets, CPUE, and catch per set. Additional variables could be included, such as FAD drift speed, vessel characteristics, and environmental variables (e.g. SST, thermocline depth).
- Additional investigation of FAD tracking and VMS data matching. For instance, this could be generalized to all vessels and years to detect FAD fishing activities during the FAD closure, to link associated fishing set and deployment with the corresponding FAD, and to follow the life history of a specific FAD through appropriation and leasing processes.
- Analyses of FAD networks could be expanded to the whole study period, bearing in mind the high computational power needed. Network analyses could further integrate catch and even other data such as tagging, to examine apparent effects on distribution at meso-scales and inform stock assessments through catchability or other parameters.
- Investigate the frequency of setting on individual FADs per vessel or fleet, in relation to the overall array of FADs available and environmental variables.
- Perform a matching between FAD sets from logsheet data and the PNA FAD tracking data to estimate coverage rates of the PNA FAD tracking data over time.

We invite WCPFC-SC15 to:

- Note this analysis on the PNA FAD tracking data and the progress being made by PNA in FAD tracking for the purpose of improving FAD management in PNA waters.
- Note the simulation method implemented to fill in the gaps in FAD trajectories and to compile corrected FAD densities maps. Furthermore, given the influence of FAD densities on CPUE, also note the key role that FAD densities may play in CPUE standardisation, but also in tuna behaviour as suggested in WCPFC-SC15-EB-WP-08. Hence, further note the importance of accessing FAD densities at the finest resolution possible for scientific analyses to guide management.
- Note the importance of complete FAD tracking data to support scientific analyses and encourage their provision by fishing companies.
- Note that findings of this paper highlighted that more than 50% of the FADs are lost to the fishing company owning it and that at least an additional 7% end up beached.

Acknowledgments

The authors would like to thank the members of the Parties to the Nauru Agreement for giving us access to their data for this analysis, and The Pew Charitable Trusts for the funding provided to support these analyses.

References

Escalle, L., Brouwer, S., Pilling, G., 2017a. Report from Project 77: Development of potential measures to reduce interactions with bigeye tuna in the purse seine fishery in the western and central Pacific Ocean ('bigeye hotspots analysis'). WCPFC Sci. Comm. WCPFC-SC13-2017/MI-WP-07.

Escalle, L., Brouwer, S., Pilling, G., PNAO, 2018a. Estimates of the number of FADs active and FAD deployments per vessel in the WCPO. WCPFC Sci. Comm. WCPFC-SC14-2018/MI-WP-10.

Escalle, L., Brouwer, S., Scutt Phillips, J., Pilling, G., PNAO, 2017b. Preliminary analyses of PNA FAD tracking data from 2016 and 2017. WCPFC Sci. Comm. WCPFC-SC13-2017/MI-WP-05.

Escalle, L., Muller, B., Brouwer, S., Pilling, G., 2018b. Report on analyses of the 2016/2018 PNA FAD tracking programme. WCPFC Sci. Comm. WCPFC-SC14-2018/MI-WP-09.

Fonteneau, A., Chassot, E., Bodin, N., 2013. Global spatio-temporal patterns in tropical tuna purse seine fisheries on drifting fish aggregating devices (DFADs): Taking a historical perspective to inform current challenges. Aquat. Living Resour. 26, 37–48. https://doi.org/10.1051/alr/2013046

Gershman, D., Nickson, A., O'Toole, M., 2015. Estimating the use of FAD around the world, an updated analysis of the number of fish aggregating devices deployed in the ocean. Pew Environ. Gr. 1–24.

Girard, C., Benhamou, S., Dagorn, L., 2004. FAD: Fish Aggregating Device or Fish Attracting Device? A new analysis of yellowfin tuna movements around floating objects. Anim. Behav. 67, 319–326. https://doi.org/10.1016/j.anbehav.2003.07.007

Harley, S., Tremblay-Boyer, L., Williams, P., Pilling, G., Hampton, J., 2015. Examination of purse seine catches of bigeye tuna. WCPFC Sci. Comm. WCPFC-SC11-2015/MI-WP-07 29pp.

Lange, M., van Sebille, E., 2017. Parcels v0.9: prototyping a Lagrangian Ocean Analysis framework for the petascale age. Geosci. Model Dev. Discuss. 2017, 1–20. https://doi.org/10.5194/gmd-2017-167

Lopez, J., Moreno, G., Sancristobal, I., Murua, J., 2014. Evolution and current state of the technology of echo-sounder buoys used by Spanish tropical tuna purse seiners in the Atlantic, Indian and Pacific Oceans. Fish. Res. 155, 127–137. https://doi.org/10.1016/j.fishres.2014.02.033

Maufroy, A., Chassot, E., Joo, R., Kaplan, D.M., 2015. Large-scale examination of spatio-temporal patterns of drifting fish aggregating devices (dFADs) from tropical tuna fisheries of the Indian and Atlantic Oceans. PLoS One 10, 1–21. https://doi.org/10.1371/journal.pone.0128023

Moreno, G., Dagorn, L., Sancho, G., Itano, D., 2007. Fish behaviour from fishers' knowledge: the case study of tropical tuna around drifting fish aggregating devices (DFADs). Can. J. Fish. Aquat. Sci. 64, 1517–1528. https://doi.org/10.1139/f07-113

Okubo, A., 1971. Oceanic diffusion diagrams. Deep Sea Res. Oceanogr. Abstr. 18, 789–802. https://doi.org/10.1016/0011-7471(71)90046-5

Scutt Phillips, J, Escalle, L., Pilling, G., Sen Gupta, A., van Sebille, E., 2019. Regional connectivity and spatial densities of drifting fish aggregating devices, simulated from fishing events in the Western and Central Pacific Ocean. Environ. Res. Commun. 1, 055001. https://doi.org/10.1088/2515-7620/ab21e9

Scutt Phillips, Joe, Leroy, B., Peatman, T., Escalle, L., Smith, N., 2019. Electronic tagging for the mitigation of bigeye and yellowfin tuna juveniles by purse seine fisheries. WCPFC Sci. Comm. WCPFC-SC15-2019/EB-WP-08.

van Sebille, E., Griffies, S.M., Abernathey, R., Adams, T.P., Berloff, P., Biastoch, A., Blanke, B., Chassignet, E.P., Cheng, Y., Cotter, C.J., Deleersnijder, E., Döös, K., Drake, H.F., Drijfhout, S., Gary, S.F., Heemink, A.W., Kjellsson, J., Koszalka, I.M., Lange, M., Lique, C., MacGilchrist, G.A., Marsh, R., Mayorga Adame, C.G., McAdam, R., Nencioli, F., Paris, C.B., Piggott, M.D., Polton, J.A., Rühs, S., Shah, S.H.A.M., Thomas, M.D., Wang, J., Wolfram, P.J., Zanna, L., Zika, J.D., 2018. Lagrangian ocean analysis: Fundamentals and practices. Ocean Model. 121, 49–75. https://doi.org/10.1016/J.OCEMOD.2017.11.008